THIN FILM COATING OF SILVER ON FIBERS BY ROLL TO ROLL INVERTED CYLINDRICAL MAGNETRON SPUTTERING

A Thesis Submitted to
the Graduate School of Engineering and Sciences of
İzmir Institute of Technology
in Partial Fulfillment of the Requirements for the Degree of

MASTER OF SCIENCE

in Materials Science and Engineering

by
Adnan TAŞDEMİR

January 2015

İZMİR

We approve the thesis of **Adnan TAŞDEMİR**

Examining Committee Members:

_____

Prof. Dr. Lütfi ÖZYÜZER
Department of Physics, Izmir Institute of Technology

_____

Assoc. Prof. Dr. Aysun AKŞİT
Department of Textile Engineering, Dokuz Eylül University

_____

Assoc. Prof. Dr. Ekrem ÖZDEMİR
Department of Chemical Engineering, Izmir Institute of Technology

22 January 2015

_____

Prof. Dr. Lütfi ÖZYÜZER
Supervisor, Department of Physics,
İzmir Institute of Technology

_____

Assoc. Prof. Dr. Mustafa M. DEMİR
Head of the Department of Materials
Science and Engineering

_____

Prof. Dr. Bilge KARAÇALI
Dean of the Graduate School of
Engineering and Sciences

ACKNOWLEDGMENTS

Firstly, I would like to thank my supervisor Prof. Dr. Lütfi ÖZYÜZER for letting possibility to complete this thesis and helping during my M.S. studies. I would like to say my special thanks to my co-advisor Assoc. Prof. Dr. Gürcan ARAL for encouragement, his instructive guidance.

In addition, I am indebted to the thesis committee members Assoc. Prof. Dr. Aysun AKŞİT and Assoc. Prof. Dr. Ekrem ÖZDEMİR for their valuable comments on my thesis.

In addition, my special thanks go to, Mutlu Devran YAMAN, Şebnem YAZICI, Metin KURT, Halil ARSLAN and Cem TÜRKAY who help me during my thesis because of their friendship and support whenever I need. I want to thank Hasan KÖSEOĞLU, Gülşah AKÇA and Hakan ALABOZ for helping me in electrical characterization, XRD-SEM analysis and optical imaging respectively.

I would also like to acknowledge that this research is partially supported by KOSGEB and Teknoma Technological Materials Inc. I would like to thank to this collaboration for providing me research opportunity.

I want to thank to Zeynep ORHAN who has a special role in my life for her unique love, infinite patience and incredible support.

Finally, I can’t find better words to explain contribution of my family to my education and explain their love. I express my thanks for their helps.

ABSTRACT

THIN FILM COATING OF SILVER ON FIBERS BY ROLL TO ROLL INVERTED CYLINDRICAL MAGNETRON SPUTTERING

There is a huge demand in functional textile product by the advent of nanotechnology and thin film technology. Antistatic and antibacterial textile materials are highly required in medical centers, clean rooms, military basis and electronic device manufacturers. Moreover, these materials are increasingly studied in many scientific committees by several method. Functional textile fabrics can be produced by surface finishing or adding conductive fibers. Many methods are employed to obtain conductive fiber but Physical Vapor Deposition (PVD) offer better homogeneity and high efficiency when compared to Chemical Vapor Deposition (CVD) methods. Magnetron sputtering is the industrial scale thin film production technique among PVD methods. However, mainly used planar magnetron sputtering systems do not enable samples to be coated all sides of cylindrical surface of a fiber so that an inverted cylindrical magnetron (ICM) sputtering system was designed for this research. ICM system was optimized and operated to deposit silver thin film on all sides of PA fibers which have diameters 85 and 150 um. A continuous roll to roll mechanism was mounted to system that enables to metalize fibers at high speed continuously. Conductive fibers are proposed to be produced at industrial scale. XRD, SEM and optical microscopy characterizations are employed on silver thin film coated polyamide fibers. In order to obtain thin film thickness of fibers, they are investigated by three different methods which can be calculating from i) bulk resistivity formula by using measured resistance, ii) deposited silver mass by using density of silver and iii) system calibration sample which is basically sending a glass lamella with same sputtering parameters and measuring sputtered thin film on it. These all results were compared to find optimum thickness. These conductive fibers woven in synthetic fabrics to promote them antistatic and shielding property. Antistatic and adhesion analysis of these fabrics are investigated and surface resistance and shielding property of fabrics were studied. All in all, these fabrics will be used as technical textile which is presumed to satisfy demands.

ÖZET

RULODAN RULOYA TERSİNMİŞ SİLİNDİRİK MIKNATISSAL SAÇTIRMA İLE LİFLERE İNCE FİLM GÜMÜŞ KAPLANMASI

Nanoteknolojinin ve ince film teknolojisinin gelişi ile fonksiyonel tekstil ürünlerine büyük bir talep olmuştur. Elektronik devre üreticilerinde, askeri birimlerde, temiz odalarda ve tıp merkezlerinde antistatik ve antibakteriyel tekstil malzemelerine büyük oranda gereksinim duyulmaktadır. Dahası, bu malzemeler bilim insanlarınca birçok metot ile oldukça fazla çalışılmaktadır. İşlevsel tekstil kumaşları yüzey işlemleri veya iletken lif eklemek ile elde edilebilir. İletken lifler eldesi için birçok yöntem kullanılabilir fakat PVD yöntemleri CVD'ye göre daha iyi homojenlik ve verimlilik sunmaktadır. Mıknatıssal saçtırma PVD yöntemleri arasında endüstriyel olarak kullanılan bir ince film üretme tekniğidir. Fakat çoğunlukla kullanılan düzlemsel mıknatıssal saçtırma sistemleri silindirik yüzeyli bir lifin yüzeyinin homojen olarak kaplanmasına olanak sağlamadığından dolayı bu çalışma için bir tersinmiş mıknatıssal saçtırma sistemi tasarımlanmıştır. Sistem optimize edilmiştir ve çapı 85 ve 150 mikrometre olan polyamid (PA) liflerin tüm yüzeylerinin homojen olarak gümüş ince filmi büyütmek için kullanılmıştır. Yüksek hızda lif metalizasyonu sağlaması için sisteme bir rulodan ruloya kaplama mekanizması monte edilmiştir. Endüstriyel ölçekte iletken lif elde edilmesi planlanmıştır. Bu sistemde gümüş film kaplanmış PA liflere XRD, SEM ve optik mikroskobu karakterizayonları yapılmıştır. Liflerin gümüş film kalınlığını bulmak için üç farklı metodlarından i) bulk direnci formülünde ölçülen direnç kullanılarak ii) teorik özkütle formülünde büyütülen gümüşün kütlesi kullanılarak ve iii) aynı parametrelerini kullanarak kaplanan ve ince film kalınlığı ölçülen cam örnek kullanılarak bulunabilmiştir. Bu sonuçlar optimum kalınlığı bulmak için karşılaştırılmıştır. Bu iletken lifler sentetik bir kumaş içine kumaşa antistatik, antibakteriyel ve elektromanyetik kalkanlama özelliği kazandırmak için dokuma yapılmıştır. Bu kumaşların antistatik, yapışma analizleri araştırılmıştır ve de yüzey direnci ile elektromanyetik kalkanlama özellikleri çalışılmıştır. Bu çalışmanın sonucu olarak bu kumaşların teknik tekstil için istenen gereksinimleri karşıladığı bulunmuştur.

To my Family

TABLES OF CONTENTS

LIST OF FIGURES

LIST OF TABLES

Table **Page**

CHAPTER 1

INTRODUCTION

According to recent reports, 25% of electronic equipment's failure occurs due to Electro Static Discharge (ESD). The 50% of devices is reported to break down due to ESD, which were working in an efficient way, formerly. The cost of the failure of materials due to ESD has assessed approximately 25 trillion dollars. ESD just needs dissimilar materials interaction and it occurs in every part of our lives. A human body can accumulate static charges on itself and they can be created even while walking on the carpet. A person walking across the floor generates static electricity as shoe soles contact and then separate from the floor surface as shown in Figure 1.1. Static charge shearing while walking on a carpet

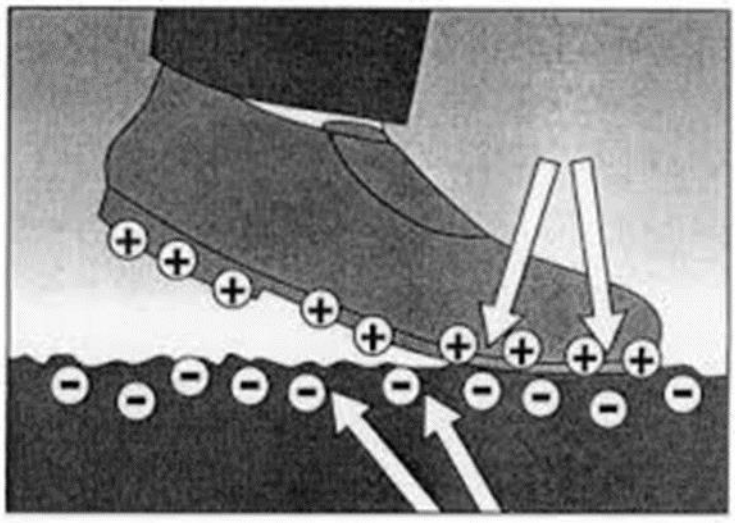

Figure 1.1. Static charge shearing while walking on a carpet
(Source: ESD interaction while walking 2001)

The static charges occur in seconds and ESD withstand voltage is the highest voltage level that the limit does not cause device failure. Many electronic components are sensitive or susceptible to ESD damage at relatively low voltage levels. Many are susceptible at less than 100 volts, and many disk drive components withstand voltages even below 10 volts. While there are thousands of volts of static charges on a body, touching a device including a sensitive transistor such as CMOS, may decrease its

lifespan, which has safe limit of 250 V. Current trends in product design and development pack more circuitry onto these miniature devices, but unfortunately it increases their sensitivity to ESD and makes the potential problem even more acute. Some degradation of the threshold voltages of the electronic circuit elements are shown in the Table 1.1. Electronic circuit elements distortion threshold voltages

Table 1.1. Electronic circuit elements distortion threshold voltages
(Source: IC threshold values, 2014)

MOSFET	100 V	**SCHOTTKY DIODE**	300 V
EPROM	100 V	**BIPOLAR TRANSISTOR**	380 V
JFET	140 V	**SRC TRANSISTOR**	680 V
CMOS	250 V	**SCHOTTKY TTL**	1000 V

It is obtained from recent researches that static charge does not discharge suddenly but it discharge slowly upon a 1 Mohm resistor. A standard discharge time is determined as 3 second. The materials using in a laboratory should not create static charges on themselves and should discharge the static charge ideally. According to the basis of this conclusion, strict precautions should be taken by using antistatic materials while interacting with electronic equipment in all environments. Surface resistance is the key factor that control the static discharge time. The surface resistance of conductors is between 10^4-10^5 ohm and they provide rapid discharge. This range is less than 10^4 ohm for shielding materials. The surface resistance of insulators is greater than 10^{12} ohm and they act as a source that generate static charges. The range between these two kind of materials refers to dissipative materials and their surface resistance is 10^6-10^{12} ohm which also include antistatic materials in range 10^9-10^{11} ohm enable materials to eliminate static discharge safely.

The antistatic materials is needed to use to eliminate the threat of static electricity. Surface resistance of static dissipative materials lay between insulators and conductors. They allow static to build up on them, while they can conduct it as well, at a slower rate than a conductor can do. Charges transfer faster than they would on an insulator, but slower than on conductors. The static charges on materials are tend to be in motion and

thus it search opportunities to encounter materials within, which it can transfer static charges. Therefore dissipating the charges is required, and this can be available by implementation of conductive materials to enable the charge to be moved safely.

There are several methods to produce these materials to eliminate ESD safely. Conductive property embedded fibers are needed to obtain antistatic textile products. Conductive nanoparticles are added in polymer fibers or metalized polymer fibers are used to promote conductive property to polymer fibers. These fibers are encapsulated in textile fabrics to obtain antistatic products. There are many studies such as surface finishing, nanoadditives in fibers and metallization of fibers corresponding to functional and smart textiles which can be seen in the literature. In these researches, antistatic, shielding properties are aimed to be studied.

Some of the fabrics made of polymeric fibers such as polypropylene (PP) or polytetrafluoroethylene (PTFE) are used in textile which are not suitable for metallization because their deposited layer poorly adheres and it is subject to wear (Ziaja, et al. 2008). According to Ziaja research, plasma activation is the only method which deposit a metal layer by evaporation. Because of rough metal layer deposition on the fiber surface, the available textile materials are not suitable for applications, because they are prone to lack of adhesion and failure of metal layer. Also, they impair further processing and functioning of the metalized textiles and there is a limited usage (only a few polyamide products) in the wet-chemical metallization of textile substrates.

So far, coating was applied to compensate the requirements of antimicrobial treatments on textiles. In this study, antibacterial silver films on poly(ethylene terephthalate) (PET) fabrics are tried to be prepared by high-power impulse magnetron sputtering technique (HIPIMS) (Chen, et al. 2013). Magnetron sputtering is one of the vacuum coating techniques and it is well developed for antimicrobial metal deposition (Dowling 2001; Baghriche 2012). Uniform coverage and modification of the surface properties of natural fiber and woven fabric materials are facilitated with atomic scale material deposition but in macro-scale interpenetrating fiber network, irregular nanoscale features are embedded. Conformal scale aluminum oxide (Al_2O_3) modified cotton textiles demonstrated extreme hydrophobic effects which are different from planar surfaces but have same coatings. This increase can be result of the increased rigidity of individual fibers because of unsuitable inorganic coating. The hydrophobicity of the fabric surface

can be increased by reduction of the total contact area between fiber and the water droplet and this reduction is result of the increase of rigidity. According to the result, reactive growth precursors are allowed due to unequal atomic layer deposition which leads to penetration through a typical woven network. This provides a highly conformal inorganic coating on folded surfaces which is mostly seen in natural textile materials (Hyde, et al. 2007). Natural plant based and protein like fibers such as cotton, linen, wool, were spinned into bundled yarns by Egyptians more than 6000 years ago in order to weave these yarns into fabrics for many purposes including clothing (Adanur 2001). But for production of advanced apparel, medical devices, military and many different purposes, new multifunctional textiles instead of traditional ones are required (Black, et al. 2005.).

In order to keep the velocity constant at 10 m.min-1, polyester multifilament (164 dtex f136) which includes 136 single filaments and a microfilament with a diameter of 0.2 mm were processed by twisting off the fiber bobbin with a sealing system in a vacuum chamber where the fiber was first cleaned by several times directing with RF plasma. For RF plasma cleaning, pressure was set as 1000 Pa (10 mbar) and He/O_2 gas flow was adjusted as 100 sccm (Hegemann, et al. 2007). Silver (Ag) metallization was performed in Inverted Cylindrical Magnetron (ICM) which performs the sputtering at 10 Pa (0,1 mbar) and 50 sccm argon (Ar) gas flow. A cylinder unit was produced with 200 mm inner diameter, 4 mm wall thickness (surface area of the target is 238.76 cm^2) and 40 mm in length. UMICORE materials with 99,999 % purity were used for production of the unit and, before leaving the vacuum chamber the coating zone was passed 72 times with the fiber. In order to achieve the film thickness which is deposited Ag quantity on the fiber and to increase ion energies in the plasma, the sputtering power was increased to 4200 W from 200 W pulsed at 100 kHz. By applying metal and insulation deposition onto the surface of elastic hollow fiber, artificial hollow fibers of the sensor were developed. Uniform deposition of the metal film on the tube surface was obtained by integrating a rotating mechanism in the sputtering equipment. For the production of rectangular-shaped tangible fabric sensor, artificial hollow fiber and conventional cotton yarns were weaved (Hasegawa, et al. 2008). Layer-by-layer deposition method was used to immobilize antimicrobial silver nanoparticles on nylon silk fibers and the deposition of these antimicrobial silver nanoparticles on fibers was controlled with number of deposition cycles (Dubas, et al. 2006). With this method, the possibility of the production of silver nanoparticle coated silk or nylon fibers was shown.

For processing and treatment of cotton fabrics, a new finishing process method was developed by pad-dry-cure method which includes different amounts of Ag-doped, Ti-based transparent solutions prepared with a sol–gel method (Onar, et al. 2007). For deposition of the surfaces of textile fabrics, plasma coatings can be used as permanent hydrophilic treatment or substrate independent staining. Addition of anti-microbial properties were facilitated with co-sputtering Ar with the silver target, and this allowed the in-situ incorporation of silver nanoparticles within functional polymers (a-C:H:N). Ag nanoparticles were distributed homogeneously at the coating surface, so by combining deposition / etching / sputtering process for plasma coating deposition facilitated the multifunctional surface formation. Web and fiber coater usage demonstrated the possibility of continuous deposition of plasma coatings on textile fabrics and fibers. Moreover, this enables industrial scale up of these textile fabrics and fibers. (Guimond 2007). Applied power and gas flow parameters is observed highly correlated with the amount and size of silver nanoparticles that used in plasma polymerization and co-sputtering. The presence and orientation of silver nanoadditives might be integrated through the monomer gas flow rate varying the plasma polymer growth rate and the integration of the particles (Körner, et al. 2011).

For the fabrication of nanostructured silver surfaces, magnetron sputtering method was applied. Nanostructured silver surfaces were treated with high purity (99, 99 %) silver target in order to deposit these surfaces onto polyester fiber. The density of silver particles deposited on the surface of polyester fibers was observed with SEM imaging after sputtering. As a result, the density of silver particles on the surface was high and the average UPF of the silver-coated polyester significantly increased. The polyester properties of the surface changed from hydrophobic to hydrophilic (CA=132.2^{o}) and silver-coated polyester gained excellent antibacterial performance with modified silver nanoparticles. These products have potential for usage in UV shielding, hydrophobic coating and antibacterial applications (Jiang, et al. 2010).

In order to increase resistance of textiles against microorganisms, and also to protect textiles from colony formation of odor-forming bacteria, antimicrobial techniques are used (Lacasse and Baumann 2004). Yoosefi et al. coated silver nanoparticles and multi wall carbon nanotubes on PAN hollow fiber by physical and chemical method, and they obtained antibacterial properties of the coating. (Yoosefi Booshehri, et al. 2013). In order to increase hygiene in clinical and sensitive environments, antimicrobials are applied

which reduces the changes for microbial colonization of textiles and their transfer from fabric surfaces (Heine, et al. 2007). The main antibacterial compounds used in textiles are triclosan, silane ammonium compounds, zinc pyrithione and silver-derived compounds (Lorenz 2012). Among silver derived compounds, nanoscale silver and silver salts offer clear potential benefits in textile by providing very low application rates. The consumption of biocide products in fibers, leather, rubber and polymers is about 1546 metric in tones and there is an increased demand for those products although there are discussions about the use of silver or nanosilver for textile products in recent years (Windler, et al. 2013).

CHAPTER 2

ANTISTATIC

2.1. Smallest Unit of Matter

It is still a confusing and challenging to understand the nature of matter and what it originally compose of. Around 2500 years ago, a Greek philosopher named Democritus was thinking about the limitation of cutting materials and he came up the idea that there must be a point where you could no longer cut something any smaller. He named the atom as the Greek word “atomos”, which means 'that which can't be split'. Democritus was right up to a point. An atom is the smallest unit of a particular kind of material. Despite this, we can split the atoms with today’s science and technology. When atom is splitted, it becomes something else. It does not represent the silver characteristic, if a silver atom is splitted. Atom is composed of basic and fundamental subatomic particles which are called proton, neutron and electron. Likewise atom, proton, neutron and electron have their subparticles, but it is not necessary to mention about them now. The limitation up to proton, neutron and electron are enough to explain what this research need. The basic components of the carbon atom is shown in Figure 2.1.

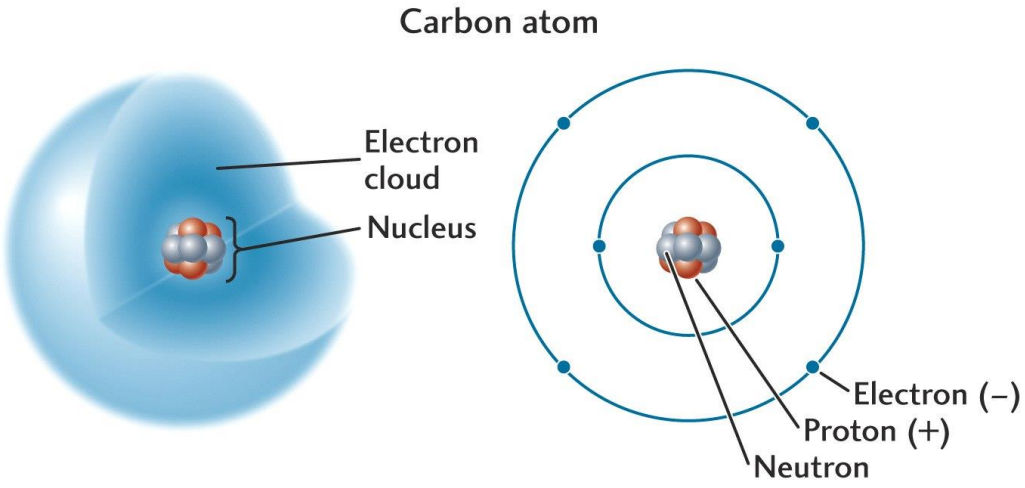

Figure 2.1. An illustration of electrons, protons and neutrons in carbon an atom (Source: Carbon atom 2013)

2.2. Electric Charge

In atoms, the electron carries a negative elementary or unit charge; the proton carries a positive charge. The two types of charge are equal and opposite. In physics, charge, also known as electric charge, electrical charge, or electrostatic charge. A positive charge comes from having more protons than electrons; negative charge comes from having more electrons than protons. A positively charged object will attract a negatively charged object. Objects with like charge repel each other and unlike charges attract one another as shown in Figure 2.2. These mutual interactions resulted in an electric force between the two charged objects. An electric field, also called an electrical field or an electrostatic field, surrounds any object that has charge.

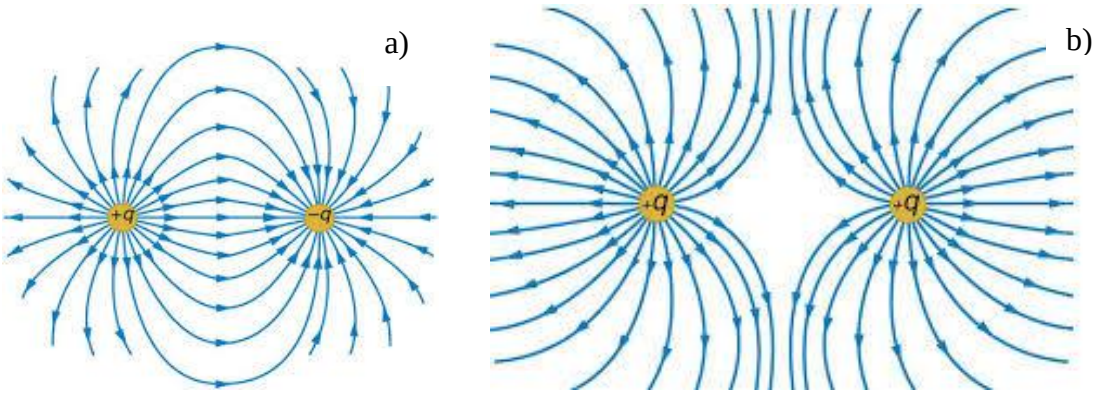

Figure 2.2. Attraction (a) and repelling (b) force of electric field between two charges (Source: E-Field lines 2013)

2.3. Electricity and Static Electricity

Static electricity and electric current are two separate phenomena. They both involve electric charge, and may occur simultaneously in the same object. All materials are made of atoms and atoms consist of electrons, protons and neutrons. Electricity creation on/in a material depends on allowance of electrons movement and their bonding properties.

Material resistance measures how well it conducts electricity. The electrostatic force can make electrons to move from one atom to another. When those electrons move between the atoms, a current of electricity is created. The movement of electrons from one atom to another is the flow of the charge as similar occurrence in a wire which can be thought the action of electricity. Electric current is the flow of electric charge through an object, which produces no net loss or gain of electric charge (Jahn 2012).

Static electricity refers to accumulation or motion of the electric charge on an object and rapid shearing with another object. This result yields the related electrostatic discharge when two objects are brought together that are not at equilibrium and the concentrations of initial charges is changed. An electrostatic discharge creates a change in the charge of each of the two objects.

2.4. Formation of Static Electricity and ESD

Electrostatic discharge can be a significant threat to electronic components, equipment and personnel, especially when working around flammable materials. The development of ways to predict the susceptibility of materials to generate significant charge is important for the safety of these personnel and equipment (Groop, et al. 2003). In nature, lightning is caused by the charging of dust and ice particles, which produce large potentials leading to electrical breakdown (Latham 1969). Similarly, volcanic lightning occurs when the ash particles in volcanic plumes triboelectrically charge and produce large electric fields sufficient for gas breakdown (Mather and Harrison 2006.). The triboelectric charging of sand or dirt in dust devils generates bipolar electric fields with potentials of several thousand kilovolts, which have the potential of damaging electronic equipment (Farrell, et al. 2004). Static electricity is generated every time materials rub against each other. A simple movement, such as a technician walking to their workbench, is enough to generate static electricity that could melt or deteriorate a device’s delicate electronic components. Electrostatic discharge (ESD) is generally known as the rapid, spontaneous transfer of electrostatic charge induced by a high electrostatic field. ESD usually occurs by rubbing, touching, or the charge flows through a spark between two bodies at different electrostatic potentials as they approach one another (Wang 2002). Static electricity occurs when the electrons on the surface of one

object pass onto another, causing it to become positively charged. The additional electrons are then just waiting for the opportunity to escape through a conductive object that allows the passing of electricity which is known as an ESD event.

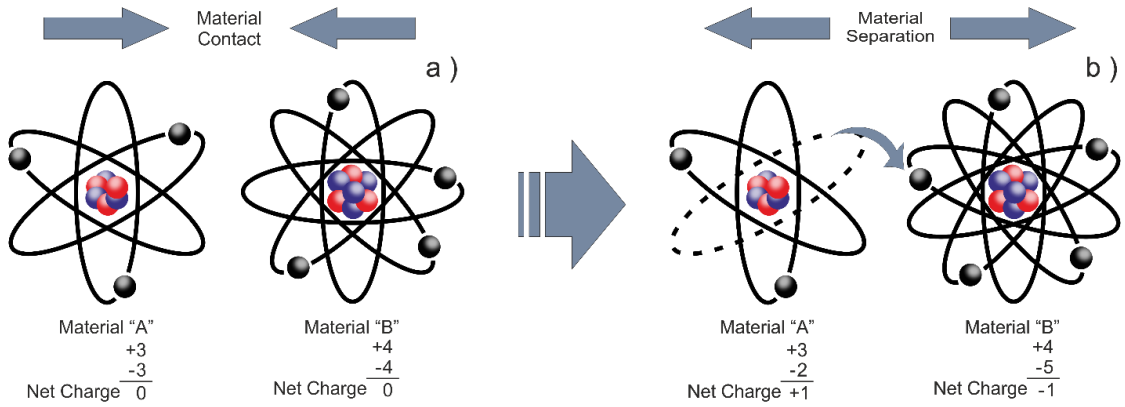

Figure 2.3. Triboelectric effect between dissimilar materials

In Figure 2.3, triboelectric effect is showed between material A and B as an example. In Figure 2.3-a, material A and material B initially consists of atoms with equal numbers of protons and electrons. They are both electrically neutral materials. When the material A and B are brought in contact and then separated, negatively charged electrons are transferred from the surface of one material A to the surface of the material B. Which material loses electrons or gains electrons will depend on the nature of the two materials. As shown in Figure 2.3. Triboelectric effect between dissimilar materials the material becomes positively charged when it loses electrons, while the material becomes negatively charged when it gains electrons.

The motion of the electrons from one material to another creates static electricity. Static electricity is measured in coulombs and equation 2.1 or 2.2 can help to be informed about charge motion on materials. The charge "q" on an object is determined by the product of the capacitance of the object "C", the voltage potential on the object (V), relaxation time of the charge transfer or discharge "t" and "β" can be called a constant:

$$q = CV \tag{2.1}$$

and

$$q = q_0 \exp(-\beta\, t) \tag{2.2}$$

All materials tend to return their original state which is ground or equilibrium state. In order to re-state ground level, they want to regain or discharge the electrons (Wang, et al. 2012). The relaxation time of gain or discharge the electron depends on related materials. The withstand voltage is depend on materials and it determine the threshold value of voltage bearing to damage caused by ESD. The loaded voltage due to transferred static charges can exceed the threshold value of an electronic devices and the devices will be no longer safe in this circumstance. These materials can be classified in two main groups such as insulators and conductors.

Insulators hold their electrons very tightly due to their bonding which is generally covalent or ionic bonding. Electrons are not allowed to move within their structure very well. For this reason, electricity cannot flow through them. Thus, gained charges stay on the surface of the insulator and remain static. Insulators are therefore highly resistive as they restrict the flow of electricity. When all the charges are focused in one area, they can lead to build-up a quite strong voltage causing damage by ESD. Mostly ceramics and polymers such as rubber, plastic, cloth, glass and dry air are good insulators and have very high resistance.

On the other hand, conductive materials are loosely held electrons, which move through them very easily. Most metals – like copper, aluminum or silver – are good conductors. Conductors have low resistance as they allow for movement of electrons within their structure meaning electricity can flow freely.

Commonly, however, we speak of the electrostatic potential on an object, which is expressed as voltage. There are many factors that may affect this charge transfer including environmental factors, physical and chemical characteristics of the materials and type of contact as described in the table below (Groop, et al. 2003).

Table 2.1. Factors that affect triboelectric charging of materials.

Factors	**Examples**
Environment	Humidity Pressure
Material	Work Function Material Transfer Surface Roughness Contamination Surface Deformation
Contact	Force of contact Area of contact Type of Movement during contact (fast or slow rubbing and simple contact)

2.4.1. Materials Failures by ESD

There are several examples of electrostatic discharge resulting in hazardous damages. In February of 2008, an explosion at a sugar refinery in Georgia (US) was blamed on the reaction between static electricity and sugar dust in a storage silo. Following the explosion six people were died, 62 were injured seriously at what was described as “a small war zone” by fire crews when they arrived (Bhushan 2011).

Figure 2.4. An explosion at a sugar refinery due to ESD in Georgia (US)
(Source: Explosion due to ESD 2011)

There have also been numerous explosions on oil tankers which is blamed on the build up of static electricity. An oil tank containing approximately 7000 barrels of diesel oil exploded while being filled at petroleum storage terminal. The total loss were over two million US dollars. It is concluded that flow rate of the material flowing into the tank was too high while the tank level was low and incoming liquid discharged into the vapor space of the tank. The high flow rate caused a static electric discharge in the tank vapor space, which contained a flammable atmosphere (Pang and Chow 2012).

In 2003, the number of fires at Japanese gas stations led to the distribution of vulcanized rubber mats along with calls for Japanese car manufacturers to replace metal fuel caps with plastic to insulate the fuel tank from ESD. In recent years, there is an increase in number of fires at gas stations and ESD from mobile phones is claimed to be responsible for it. Prior 2000 to 2005, 243 gas station fires have been pointed to mobiles, but now experts declare that the reason is not mobiles but static electricity (Martinez 2014). It's believed that the main reason fires occur at gas stations is because of the static generated when people get back into their cars, rub against the seats and then release the static discharge when they return to the fuel pump.

2.5. Antistatic

Static electricity has become a major problem in our daily life and especially in electronics industry. By the advent of nanotechnology, devices are getting smart but also becoming smaller and sensitive. Nanotechnology lowered the devices threshold values and ESD became more hazardous to electronic equipment especially to circuitry and expensive devices. World needs smart and functional textile product to handle these developments in high technology. Thanks to antistatic property, there are several applications to prevent undesirable results of ESD. Effective ESD control applications require a variety of procedures and materials.

Antistatic property enables materials to eliminate ESD by controlling dissipation static charge on their surface safely (Özyüzer 2010). Charge Dissipation is the process by which excess charge is neutralized. Static charge which is accumulated on the surface of materials creates voltage and this voltage can be greater than materials threshold level. By lowering the number of accumulated static charges and controlling the relaxation time

for static charges on surface, materials can block the hazards due to instantaneous ESD. In order to reach this purpose, materials need to be added conductive properties according to the surface resistance range of antistatic materials. They should be functionalized and their surface resistance range should lay between at least conductive and insulator materials.

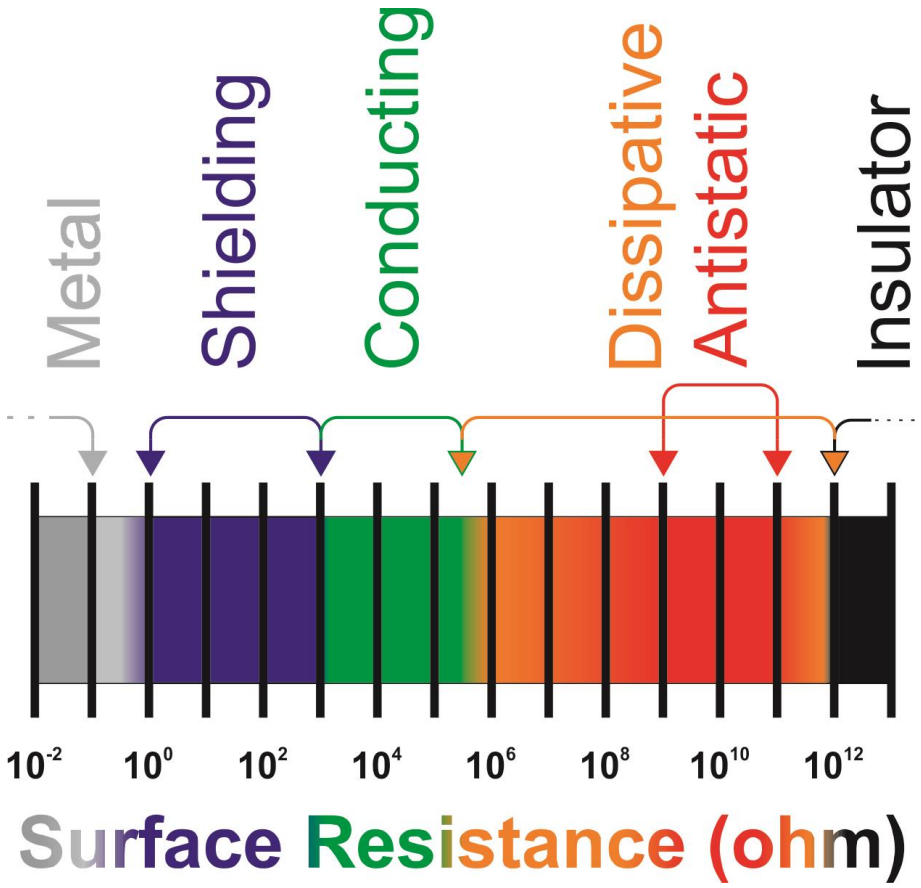

Figure 2.5. Surface resistance of antistatic fabrics

2.6. Antistatic Applications

Antistatic applications offers strick precuations to eliminate ESD denger for many part of life and safety of electronic devices. There are many examples such as antistatic shoes, antistatic floor covering, antistatic socks. Most popular applications are as followed

The aim for the military sector is functionalization of the textile about integrated electronics into **military dressings** (Figure 2.6-a). Desired smart clothes are suitable for wearable computing equipment but it is not really possible. If it could be accomplished, soldiers can find easily their partner's position and commanders can give directions to the soldiers. Despite all them, durable and comfortable clothing can be possible for a specific thermal signals to detect soldier position. In addition, antistatic military clothing enable to emit same thermal signal from all part of body. So, human body will look like as there is no living thing because human body normally emits different thermal signals from different part of body. It will be an advantage for alliance side but a disadvantage for opponent side.

There occurs several crucial operation in surgery rooms so that these rooms is equipped by sensitive devices that monitor and measure the crucial process of human life. Surgery rooms need useful textile products and functional uniforms to eliminate to eliminate danger of ESD problem. Environment sterilization in surgery room is another factor that should be paid attention. Dirt and humidity can also lead ESD events and they are both harmful to patient and electronic equipment. The electrostatic charges accumulating on the surface of filtration media are major fire and explosion hazards. The danger is eliminated when static-reducing or conductive fibers or yarns are added to the filtration media. The effectiveness of such materials is determined by comparing the equivalent energy of potential discharges with the minimum ignition energy of the inflammable atmosphere. Furthermore, **surgery room clothes** (Figure 2.6-b) and **filtration** are widely used and they play important role in hospitals. Besides the antistatic property, these textiles should be added antibacterial property in order to prevent patient from any microbial effects.

Dealing with the high technology needs sensitive measurement and expensive devices during the production and characterization of new devices. Clean rooms is equipped with sensitive and expensive devices. It is important to produce sensitive devices as much as to be sure of sensitive measurements. Nanotechnology production sample is at the range of nanometer and they are more tend to static charges and ESD events. **Clean room garments** (Figure 2.6-c) are used to prevent any harmful damage caused from electronic equipment or working people to samples at clean room.

Figure 2.6. Some Antistatic applications
(Source: Meriç 2011)

Electromagnetic (EM) Shielding (Figure 2.6-e) can be provided by antitatic application to prevent electromagnetic radiation which is dangerous on people, plants and animals. Textile materials which are electrically conductive can be used as shielding to protection against electromagnetic fields. Electronic equipment can be lost efficiency or damaged by different frequencies of radiation. Electrically conductive textiles is gained shielding property in order to prevent harmful effects of electromagnetic waves. Governments, hospitals and banks secret systems or data basis can be protected by antistatic electromagnetic shielding. Antistatic rain-wear be protected from external fields that spying information systems. This application can be used for mobile phone also. The smaller electromagnetic wavelengths are more harmful to human body (Wessapan, et al. 2011). At these energies electromagnetic radiations are X and gamma rays and they are more energetic. When they strikes on molecules, molecules ionize and this cause defects in the molecule structure that cause harmful biochemical reactions. The cancer formation can be resulted by these reactions effect. Specific Absorption Rate (SAR) refers that EM

radiation which causes the 1 ^{o}C increase human body temperature is harmful. It can be concluded that antistatic textile protect from harmful radiation (Bhat and Kumar 2013).

Antistatic **and conductive bags** can be used in order to carry or store electronic devices without the risk. These materials guarantee the sensitive devices shipping properly to customers. The main ESD function of these packaging and materials handling products is to limit the possible impact of ESD from triboelectric charge generation, direct discharge, and in some cases electrostatic fields. In addition to that, these are also very suitable for electromagnetic field shielding.

Antistatic **Wristband** can made of metal or textile. In order to ground themselves, people should use wristband especially when they are working with electronic devices. Primary aim of wristband is to ground personally. There can be no hazardous discharge between them, because the person and other grounded objects in the work area are at or near the same potential. In addition, static charges are removed from the person to ground and there cannot be accumulation of static charge.

Antistatic **heel strap** are used as an alternative to antistatic shoes. They are used by employees and visitors in order to ensure the static electricity to be grounded in a work place. **Antistatic seats** can be used in many sectors such as chemical, medical, pharmaceutical, oil and military industry, hospital clean rooms and manufactory which produces electronic devices. Antistatic seats are smart textile products and they eliminate ESD events. They consist of special conductive fibers so static electricity discharges by using conductive fibers. **Antistatic gloves** (Figure 2.6-d**)** are used by sensitive electronic devices manufacturer. Small and miniature integrated circutary devices are very vulnerable to ESD if antistatic precuations were not taken.

2.7. Fabrication Methods of Antistatic Fibers

Antistatic applications can be obtained by several methods such as thin film technology, using additives, melt components, metal fibers utilization and surface finishes (Meriç 2011).

2.7.1. Metal Fibers

Metal fiber diameter and length can change according to the property being proposed to gain. Metal has perfect reflectivity property due to their nature so they can be used for electromagnetic shielding. But to obtain the antistatic property, conductive fibers should be woven into the fabrics at regular intervals. Although diameter of these fibers are very small, antistatic fabric will be heavy. They are not feasible, because heavy fabric will weight researches movement. Metal fibers have high mechanical strength but they are not as elastic as polymers. There is another reason which makes metal fibers not to be preferred is that they are expensive.

Figure 2.7. Antistatic fabric by using metal fibers

2.7.2. Bicomponent Fibers

With this method, a number of continuous fiber are extruded from a specific polymer. Another polymer can be employed in this continuity according to desired property (Kaynak and Babaarslan 2011). A single conductive fibers flow into these extrusion during the production Fibers produce casually by this method and just some of produced fibers carry desired property. Besides, these fibers are decomposable and resolvable. Obtained fibers diameters are not same and fibers diameter are not homogenous as in Figure 2. 9 (Supuren 2007). Good conductivity cannot be obtained by this method because fiber diameter are not homogenous during its longitudinal. Bicomponent are not a good method to reach antistatic property.

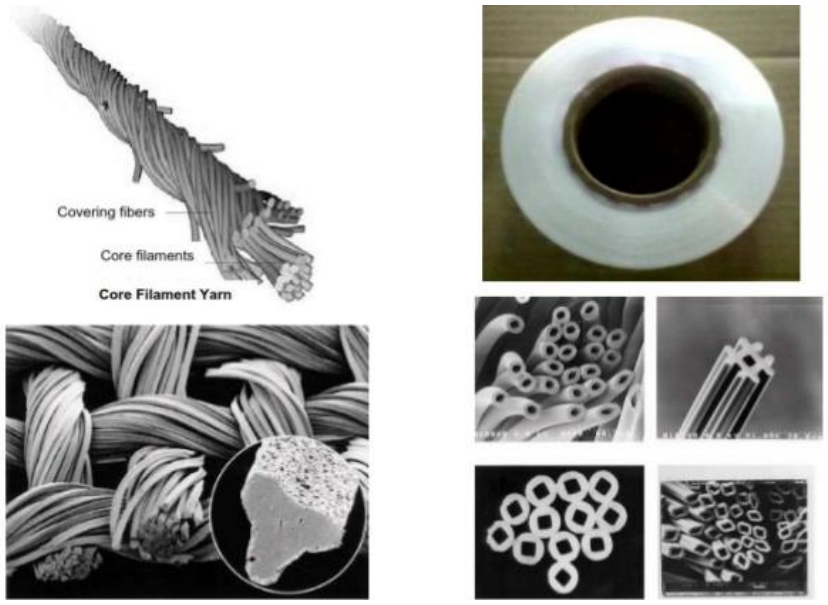

Figure 2.8. Bicomponent fibers

2.7.3. Melt Compounding Method

This method is generally preferred for polymer nanocomposites productions. The conductive nanoparticle additives are employed in a polymer solution with mass ratio calibration by this method (Zhang, et al. 2004). These conductive additives randomly distributed in the polymer fiber. The conductivity of fiber is provided by these particles. Casual orientation of conductive additives in the polymers lead lack of the continuity of conductivity. Nanoparticle dispersion is found to be unsatisfactory, and the nanoparticles is caused severe catalytic degradation on the host polymer (Chandra, et al. 2011). This method does not match to obtain antistatic property, as long as homogeny orientation of conductive additives in polymer is not provided. Because lock of conductivity leads lack of antistatic property.

2.7.4. Chemical Methods

Chemical methods such as wet chemical deposition, electroless deposition or sol-gel can be used to get conductive thin film formation on a polymer surface. They are generally used surface finishing. Chemical solutions and additives are employed during these methods not only in production part but also in sample preparation part (Textor 2010). Several chemicals are wasted during the fabrication of antistatic fibers. These all chemical can react in a different result and harm the sample surface resulting in change of sample property. If polymer fibers with small diameter is used as a sample, damage on its surface due to the chemicals would lower the tensile strength of fibers so they would not be feasible to produce antistatic fabrics. It can be concluded that this method is not suitable for coating polymer fibers with small diameter.

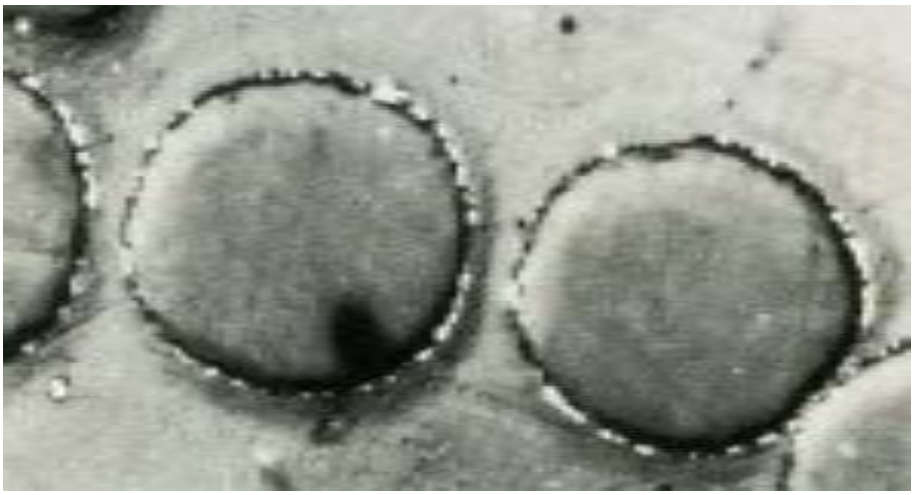

Figure 2.9. Impact of chemical on sample surface

2.7.5. Metallization of Polymer Fibers

Metallization of polymer fibers by thin film is scaled at the range of nanometer and can be obtained by thin film technology. Metallization of fibers refer to metal thin film deposition on polymer fibers in order to facilitate them conductivity property (Figure 2.10). In addition, Metals have perfect reflectivity property and do not allow light passing through. Metals such as silver (Ag) or aluminum (Al) are employed to give fabrics significant properties. When fibers are gained conductive property by coating metal, they can be woven into fabrics and fabrics are gained antistatic property.

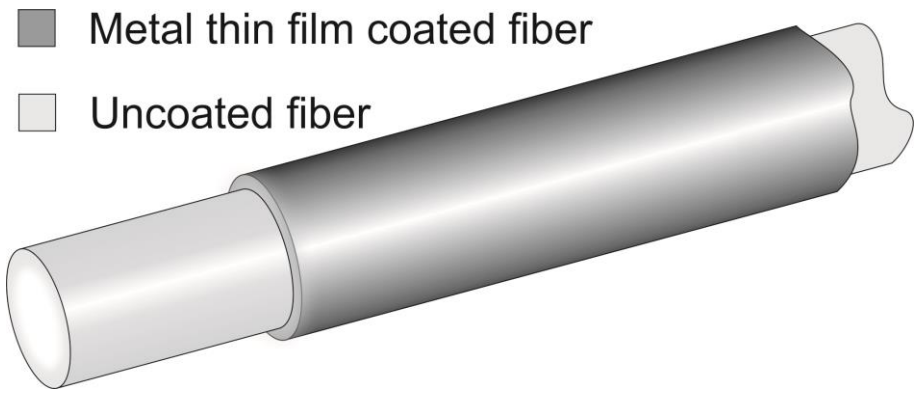

Figure 2.10. Metallization of a Polymer Fiber

The popular method is adding conductive fibers at regular intervals of functionalized textile. Surface is gained electrical property by this method. Antistatic property can be controlled by the controlling the distance between horizontal and vertical intervals.

CHAPTER 3

PHYSICS OF THIN FILMS

3.1. Definition

Thin Film: A thin film is a layer of material on a substrate ranging from a nanometer (monolayer) to a few micrometers in thickness. There are many applications of thin film such as microelectronics, electrical conductors, electrical barriers, diffusion barriers, sensors (magnetic, gas), optoelectronic devices, corrosion protection, wear resistance. The thin film technology is rapidly advancing not only due to its applications in a wide variety of areas such as the microelectronics, medical and military industries, but also due to the high demand for smart and sustainable materials for our everyday life. There are several methods for coating of polymer fibers by thin film technology. These methods separate into branches of vacuum or nan-vacuum media processing but mainly differentiates as physical and chemical methods. Many of these techniques do not obey mass production because they fit laboratory scale production for researches (Kern 1991). The disadvantages of chemical methods were mentioned before, so that physical methods are preferred to be focused in this research. Physical methods use the glow discharge plasma for thin film formation.

Thin Film production Methods (Chemical methods,* Physical Methods*)

Vacuum Thin Film Deposition Methods

- Physical vapor deposition (PVD)
  - Evaporation
    - Thermal (Resistive)
    - Electron Beam
  - Sputtering
    - Dc (Diode)
    - Triode
    - Microwave Assisted
    - Magnetron
      - Bias
      - high power impulse
      - Inverted Cylindrical
    - Rf
    - Collimated
    - Ion Assisted(Ionized Sputtering) Deposition
    - Ion Beam Sputter Deposition (IBSD)
    - Reactive
- *Chemical vapor deposition (CVD)*
  - *Atmospheric Pressure CVD*
  - *Low pressure CVD*
  - *Plasma enhanced CVD*
  - *Thermal CVD*
  - *Laser-enhanced (LECVD*)
- Epitaxial deposition
  - MBE (molecular beam epitaxy)
  - *MOCVD (Metal-Organic CVD)*
- *Electro-deposition (electroplating)*
- Atomic Layer Deposition
- Pulsed Laser Deposition
- …..

Non-Vacuum Thin Film Deposition Methods

- Electroless Deposition
- Sol-Gel
- Dip Coatings
- L-B (Langmuir-Blodgett) Technique
- Spin Coating
- Spray Pyrolysis Deposition
- Screen Printing
- Wet Chemical Deposition
- ....

Figure 3.1. Thin film deposition methods

3.2. Plasma

Chemically reactive plasma discharge are increasingly used for functionalizing the surface of the material and developing their properties. The world's largest manufacturing industries gain several advances by using plasma processing technology. Surface treatment which is based on plasma processing technology largely feasible for integrated circuits used by the electronics industry (IC) or other process such as, textile, aerospace, automotive, food, a pot for biomedical and hazardous waste management industries. Materials and surface structure can be manufactured that can't be reached by any commercial manner, and the surface properties of materials can be modified in unique ways.

Plasma is the fourth state of matter and averagely electrically neutral. It is basically a collection of free and randomly moving charged particles which composed of atoms or molecules releasing their electrons to become positively charged particle as ions and negatively charged electrons are free to move around. By increasing the temperature or directly raising the energy levels of molecules of gas, a great number of atoms are ionized, so that, it enters plasma state. Plasma state stays in equilibrium, because number of positively and negatively charged particles stay nearly equal. The aurora borealis (or the northern light), neon signs, fluorescing lights, the solar corona and glow discharges can be given as good examples of well-known plasmas. The parameters to define a plasma in numbers are temperature (energy), electron density and particle density or neutral atom density. In cold plasma, typically most of thin film processes deal with particle energy of a few eV whereas in hot plasma, nuclear fusion and some astrophysics have particle energy of a few thousand eV. In plasmas, electron temperature is generally greater than ion temperature (Chapman 1980). Glow discharges have the following features;

1. They are driven electrically.
2. Charged particles collision with neutral gas molecules are important.
3. There are boundaries at which surface losses are important.
4. Ionization of neutral sustains the plasma in the steady state.
5. The electron are not in thermal equilibrium with ions.

The fractional ionization of a plasma is

$$X_{iz} = \frac{n_i}{n_g + n_i} \tag{3.1}$$

Where n_g is the neutral gas density, X_{iz} is near unity for full ionized plasmas and n_i is charged particles density in plasma. Because these discharges are electrically driven and are weakly ionized, the applied power preferentially heat the mobile electrons, while the heavy ions efficiently exchange energy by collisions with background gas. Hence $T_e >> T_i$ $X_{iz} << 1$ for weakly ionized plasma. Low pressure discharges are characterized by T_e ~ 1-10 V. $T_i >> T_e$ and $n = 10^8 - 10^{13}\ cm^{-3}$. High pressure arc discharge are also used for processing. These discharges have T_e ~ 0.1-2 V. $T_i \leq T_e$ and $n = 10^{14} - 10^{19}\ cm^{-3}$. However, the energy of ions bombarding on thin film target can be 100 V – 1000 V which is highly exceeding T_e.

3.3. Atomic Collisions

There are several instance occurring during the two particle collision. Their momentum or energy may change by resulting that neutral particle may become ionized, and ionized particles can be neutral via this collision (Lieberman and Lichtenberg 1994). During electron-atom collision, the electron momentum is changed as an elastic process and excitation and ionization occur as inelastic process. On the other hand, in collision of ion and atom, momentum and energy are exchanged as elastic process and resonant charge transfer. There are some other process occurring in molecular gases such as dissociation, dissociative recombination, processes involving negative ions, such as attachment, detachment, and positive-negative ion charge transfer, and processes involving excitation of molecular vibrations and rotations.

Ions and electrons possess only kinetic energy. Atoms or ions have internal energy level structures and can be excited, deexcited, or ionized, owing to change in potential energy. If there is no change in the internal energies of the collisions then the sum of the

kinetic energies is conserved and collision is elastic. If the sum of the kinetic energies is not conserved, then the collision is inelastic involving excitation or ionization.

For example, an electron collision with argon atom can excite the atom (Ar*) to a higher energy level,

$$\mathrm{e} + \mathrm{Ar} \rightarrow \mathrm{Ar}^{*} + \mathrm{e} \tag{3.2}$$

This process corresponds to a change of state such as;

$$3\mathrm{p}^{6} \rightarrow 3p^{5}4\mathrm{s}^{1} \tag{3.3}$$

Atoms can be excited from their ground states to higher energy bound state by collisions or radiation. Mostly, only a single valence electron is excited. Most bound states can emit a photon by electric dipole radiation and return to some lower energy state or to the ground state:

$$\mathrm{e} + \mathrm{Ar} \rightarrow \mathrm{Ar}^{*} + \mathrm{e} \rightarrow \mathrm{Ar} + \mathrm{e} + \hbar\omega \tag{3.4}$$

The radiation is usually in the visible or ultraviolet. The radiation can be emitted by a transition between electronic levels, between vibrational levels of the same electronic state, or between rotational levels of the same electronic and vibrational state; the radiation lies within the optical, infrared or microwave frequency range respectively.

When a positive ion collide with an atom, a valence electron is transferred from the atom to the ion. In generally, the energy due to the electronic state of electron which is released is not equal to the energy of electron which is captured so the collision is not elastic. As illustration, a resonant situation is showed below:

$$Ar^{+}(fast) + Ar^{+}(slow) \rightarrow Ar^{+}(fast) + Ar^{+}(slow) \tag{3.5}$$

Although the ion and atom change their internal states, their kinetic energies are conserved. For the reaction shown in 3.6,

$$A^+ + B(at\ rest) \rightarrow A + B^+(at\ rest) \tag{3.6}$$

collision is not elastic.

If the ionization potential of the ion is greater than the electron work function, new electrons can be emitted into the gas.

$$KE = \hbar\omega - BE - \emptyset \tag{3.7}$$

BE is generally called the binding energy of the electron. Ø is the work function of the solid when KE is the Kinetic energy incoming gas species in 3.7.

Table 3.1. Others phenomena's may occurs during atomic collisions

Event	**Example**
Negative ion	$A + e \rightarrow A^-$
Dissociation	$e + AB \rightarrow A + B + e$
Dissociative ionization	$e + AB \rightarrow AB^+ + 2e$
Dissociative ionization(via *Electron ion collision*)	$e + AB \rightarrow A + B^+ + 2e$
Dissociative recombination	$e + AB \rightarrow A + B^*$
Dissociative electron attachment	$e + AB \rightarrow A + B^-$ **or** $e + AB \rightarrow A + B^{*-}$
Polar Dissociation	$e + AB \rightarrow A^+ + B^- + e$
Electron impact detachment	$e + A^- \rightarrow A + 2e$ **or** $e + AB^- \rightarrow AB + 2e$
Resonant Charge Transfer	$A^+ + A \rightarrow A + A^+$
Nonresonant Charge Transfer	$A^+ + B \rightarrow A + B^+$
Positive and Negative Ion Recombination	$A^+ + B^- \rightarrow A + B^*$
Deexcitation	$e + AB^* \rightarrow AB + e$

3.4. Nucleation and Growth

Thin film can be grown on the surface of a suitable specimen by exposing atomic flux coming from a sputtering target. In a vacuum environment, molecules or atoms with a momentum can be absorbed onto the surface and this process has two stage. Any of this particles approaching the surface of the specimen are interacted with the surface atoms. If the energy from momentum is lost by this interaction, sputtering atoms may not have energy to escape from the surface and they are physically trapped on the surface which is called the process of physisorption. Physisorption is physical adsorption including weak bonds such as Van der Waals type related energy 0.01 eV. The molecule is still able to diffuse across the surface and may either desorb if it gains sufficient energy. Otherwise, it may interact with other surface atoms to form chemical bonds – this process is known as chemisorption. Chemisorption is chemical adsorption including such as strong bonds chemical bonds type related energy 1 - 10 eV. Absorption is the process in which a fluid is dissolved by a liquid or a solid (absorbent). Adsorption is the process in which atoms, ions or molecules from a substance (it could be gas, liquid or dissolved solid) adhere to a surface of the adsorbent. Adsorption is a surface-based process where a film of adsorbate is created on the surface while absorption involves the entire volume of the absorbing substance. The term sorption encompasses both processes, while desorption is the reverse process. The surface diffusion step is very important to provide an adsorbed atom sites to find the lowest energy. There are simply three types of thin film growth for initial nucleation as shown in Figure 3.2. In Layer (Frank – van der Merwe) growth, the incoming atoms or molecule are weakly attracted each other but strongly to the substrate therefore growth is completed on an entire layer before starting to form a new one. Epitaxial growth works in this principle of thin film growth. If the incoming atoms bond more strongly with each other than with the specimen, then island shaped (Volmer-Weber) growth results with the atoms forming 3 dimensional nuclei. A mixture of the two types is also possible, as the energy associated with successive layers changes. This leads to a mixed type which is called Stranski-Krastanov.

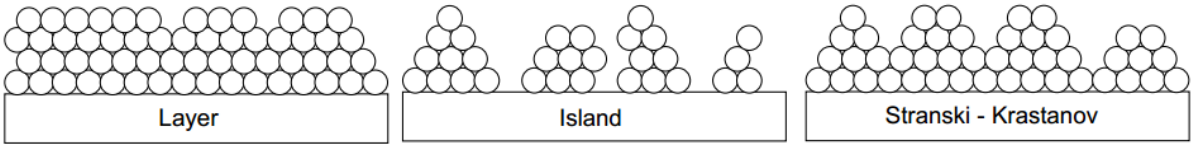

Figure 3.2. Illustration of the different thin film growth modes

3.5. The Elements for Thin Film Formation

3.5.1. Thin Film Production Requirements for PVD

• Vacuumed environment (Chamber, Flanges, Vents, Valves, o-rings, Cascades, etc…)

• Vacuum measurement tools (TC or CC gauges, Baratrones,)

• Pumps (Mechanics, Turbo Molecular, Ion, Diffusion, Cryogenic, etc…)

• Gas tubes (Argon, Oxygen, Nitrogen, etc…)

• Power Supplies (Target related)

• Some Controller Devices (for additional devices)

• Target (Sputtering source)

• Specimen (Metal, Ceramic, Polymer, Composites, Thin film Coated samples)

3.5.2. The Elements Controlling Growth Mechanism

– Substrate

–Base pressure (or contamination level)

–Deposition temperature

–Deposition rate

–Later processing temperature

–Process pressure (# collisions)

3.6. Deposition on Sample

Vacuum ambient is obtained in a suitable reservoir such as vacuum chamber including all tools above. A discharge gas is introduced as a media to ignite a plasma. The flowed gas is generally inert to prevent the unwanted reactions with the target source, however, this gas can also contain a reactive gas according to required formation of desired film. Argon (Ar) is the most common gas in sputtering processes. Argon has first ionization potential 15.7 eV and second ionization potential 27.76 eV. At 1 mtorr at room temperature, the mean free path for argon is about 8 cm but this distance is also related to electric and magnetic field line interactions beside pressure and temperature. Nitrogen (N_2) or oxygen (O_2) can lead a reactive sputtering when they are introduced the ambient with Argon. Due to potential difference between anode and cathode, an electric field is then applied between the sputtering source (cathode) and an anode. Often, the chamber wall is used as anode in the system and electrically grounded. In addition, cathode is applied negative voltage and that makes electrical field direction is respectively from anode to cathode. Even at room temperature, the gas will contain a small amount of ions and some free electrons so as our gas tube (from background radiation). When gas is flowed into vacuum chamber, electric field accelerate the ions and electrons towards the cathode and the anode respectively. The electrons then lead the formation more ions and electrons by collisions with the gas atoms. In addition to that, new electrons are also generated at the cathode surface. At a few angstroms distance from target, electrons can tunnel from the cathode to ions and the ions become neutralized. When an ion is neutralized, the energy corresponding to the ionization energy of the ion is released. This energy can then be given to a surface electron, via an Auger process. If energy transfer is high, atom will ionize and be accelerated toward cathode. These electrons are called secondary electrons. Electrons are then accelerated by the electric field, and generate new ions and free electrons. By the addition and acceleration of new electrons. An “avalanche” of ionizations has started .If the applied power is sufficiently high, a plasma is created. This process is called plasma breakdown. The plasma then adjusts itself regarding temperature, density, and distribution in space until it reaches a balance between charge losses and supplied energy. Electrons may collide with neutral species. If energy transfer is less than ionization potential of gaseous species, atom can be excited to an energetic

state. The atom decays from excited state through optical transition, providing glow (Venables 2000).

3.7. The Mean Free Path

The mean free path is the average distance between atomic collisions in a gas phase. It decrease with increasing of pressure because of increasing of number density of gas molecules. According to kinetic theory, there occur no interaction between gas atoms other than during collisions. The atomic size of gas molecules vary from gas to gas and the higher atomic size increases the probability of collisions and decreases the mean free path. In addition, the proportion of energy transfer is related to atomic collision and mean free path. According to these information, particles directly move in a straight line in a unit distance of mean free path and there is no force exerting on them in within this unit. Equation of mean free path practical units where;

P = pressure in torr and λ will be in cm.

$$\lambda = \frac{5x10^{-3}}{P} \tag{3.8}$$

1 mtorr makes mean free path 5 cm.

Therefore, as typically target-substrate has large separation, sputtered atoms have to go through tens of collisions before reaching the substrate. This reduces deposition rate considerable materials are deposited onto chamber walls. Too many collisions also prevent ionization resulting the decrease in ion density and deposition rate. High amount of the gas flow also gives same result. Equation 2.11 gives us for rms velocity of molecules;

$$v_{rms} = \sqrt{\frac{3kT}{m}} \tag{3.9}$$

k = Boltzmann's constant, T = temperature of the gas, m = mass of the molecule. The hotter it is, the faster they move. The lighter they are, the faster they move. At room temperature Ar has v_{rms} value that equals to 380 m/s.

3.8. Sputtering Yield

Sputtering yield is basically the number of sputter atoms ejected per impinging ion. Sputter yield (Y): the number of sputtered atoms per impinging ion. The sputter yield depends on the energy of the incident ions, the masses of the ions and target atoms, the binding energy of atoms in the solid; and the incident angle of ions. Mathematicall formula can be expressed as in 3.10.

$$Y = \frac{sputtered\ atoms}{bombing\ ions} = a\frac{M_1 M_2}{(M_1 + M_2)^2}\frac{E_1}{U_2} \qquad (3.10)$$

M_1: Mass of target atom

M_2: Mass of bombing ion

E_1: Kinetic energy of bombing ion

U_2: Bonding energy of target material

α: incident angle

3.9. Thin Film Production Methods

3.9.1. Chemical Vapor Deposition (CVD)

This method has very important role in semiconductor industry to produce high quality thin film. A volatile and reactive gas is flowed into a chamber and gas is chemically react with the solid sample on a nonvolatile solution placed on the sample.

System is proceeded at elevated temperatures because film occurs on the heated substrate. This method enables to deposit materials which are difficult to evaporate. Likewise physical vapor deposition, chemical vapor deposition has sever modes such as Ultrahigh Vacuum CVD (UHVCVD), Atmospheric Pressure CVD (APCVD), Plasma Enhanced CVD (PECVD), Laser Enhanced CVD (LECVD), Atomic Layer CVD (ALCVD), Metal Organic CVD (MOCVD) etc…

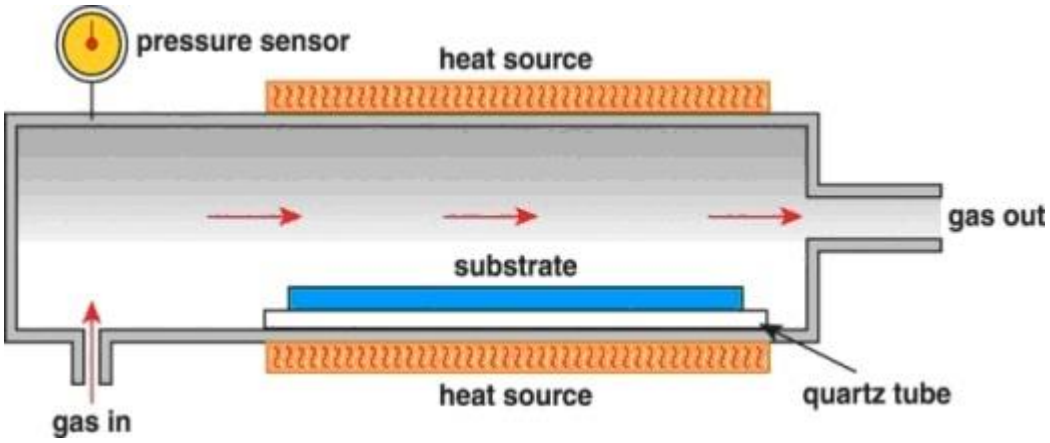

Figure 3.3. Basic principle of CVD
(Source: CVD method 2014)

3.9.2. Fundamentals of Some PVD Methods

3.9.2.1. .Evaporation

When thermal energy supplied to the crucible or boat to evaporate atoms evaporation process takes place. In this process, evaporated atoms stick to the sample after traveling through the evacuated space between the source and the sample. After sticking, there is very little rearrangement of the surface atoms and surface reactions usually occur very rapidly. Thickness uniformity and shadowing by surface topography, and step coverage are issues

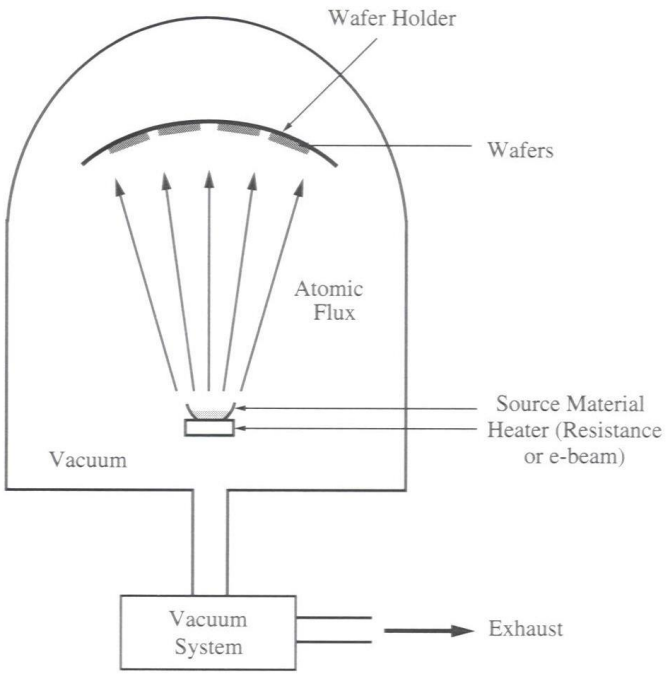

Figure 3.4. Evaporation
(Source: Evaporation 2011)

3.9.2.1.1. Thermal (Resistive)

The material of the future coating is heated by using resistance up to the evaporation temperature in the easiest case. In order to hold the evaporant materials wire basket and dimpled boat are used. Since they have higher evaporation points tungsten or tantalum are generally used as boat. A film is produced by the movement of atoms towards the substrate by a straight trajectory and depositing on it. In this case, only metals and metal alloys with a low melting points can be applied (for example, Zn, Au, Al, etc.). In evaporation process various technology is used such as metallization of fabrics.

High contamination level, not working on composite films and limited choice of materials are the major issues. High contamination: the crucible is heated as well, so may deposit to the substrate. On the contrary, e-beam evaporation heats only the evaporate material from the top.

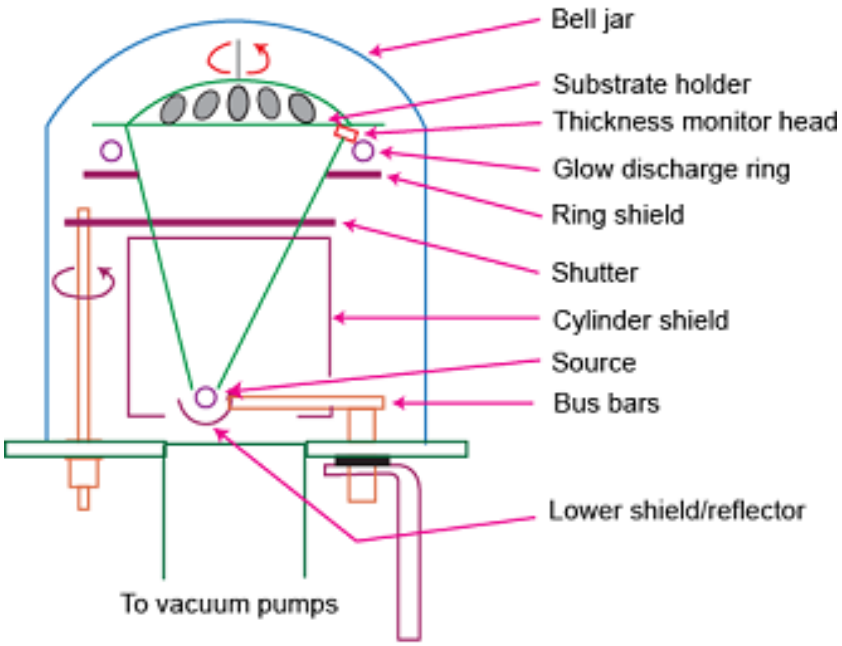

Figure 3.5. Thermal evaporation
(Source: Thermal evaporation 2014)

3.9.2.1.2. Electron-Beam

The coating material is ablated (i.e. material is removed by vaporization, bypassing the liquid phase) by using a focused electron or laser beam at a small spot at the target which is made of the coating material. Electron temperature can be as high as 10,000 K. which is appropriate for metals that have high melting temperature like W, Ta. On the source surface, evaporation takes place at a highly localized point and consequently very small contamination from the crucible occurs. All metals and metal alloys, as well as ceramics and polymers, can be used as coating materials, in contradiction to thermal evaporation, however with a low temperature process which could be as low as room temperature.

Composite films can be deposited using dual e-beams with dual targets. The improvement of thickness uniformity can be attained by substrate rotation. The high cost of the equipment (electron beam gun or laser) is the basic disadvantage of this method Issues: radiation damage; not suitable for organic materials. This method is applied, for

example, for magnetic data storage media production, but for ultra-high rate alumunization of fabrics and transparent barrier coatings, as well.

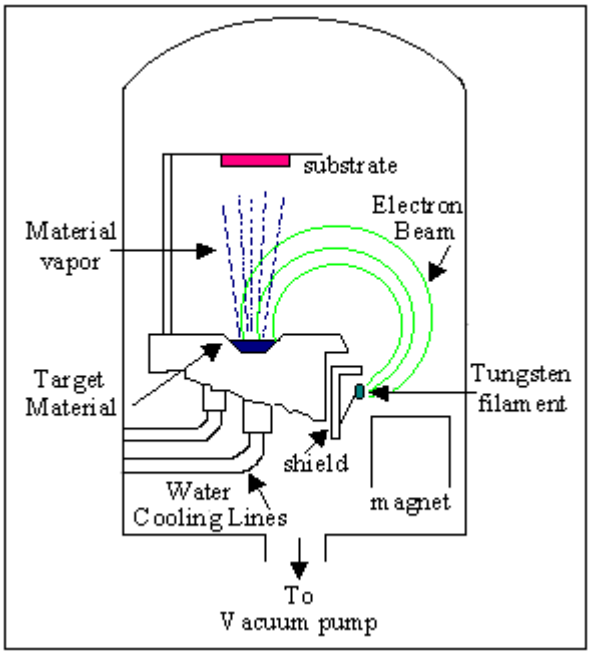

Figure 3.6. e-beam evaporation
(Source: e-beam evaporation 2014)

3.9.2.2. Sputtering

3.9.2.2.1. DC Sputtering

The sputtering process is basically manipulating target atoms to a proper specimen by a glow discharge occurring between anode and cathode. A large negative potential applied to the cathode and the anode is generally grounded. Plasma is formed after a gas is flowed into system and a sharp decrease in voltage occurs after plasma formation because plasma is a high electrical conductive form. High ion bombardment to target surface takes place and remove surface atom. By ion-atom collisions, there occur secondary electrons and these electron sustain the plasma formation by contribution to ionization process. However the majority of the electrons produced will not be involved in collisions but instead escape to the anode, making the process rather inefficient (Tuna 2010).

3.9.2.2.2. Magnetron Sputtering

Ionization rate which is number of collision between electrons and ions is low in DC and AC sputtering. Electrons energy mostly diminish without participating ionization process and dissipate via absorption by electrodes. RF field oscillations increase ionization rate barely, so that deposition rate is not efficient. In magnetron sputtering, magnets are used to increase the number of electrons participating in ionization process and resulting in increase of deposition rate (Powell and Ulman 1999). Strong magnets are positioned behind the target to form magnetic field in order to meet right angle with electric field. Magnets are aligned in such a way that one pole is placed at the center of the reverse surface of the target and the counter pole is put in ring shape order around the outer edge of the reverse surface of the target (Francombe and Vossen 1992).

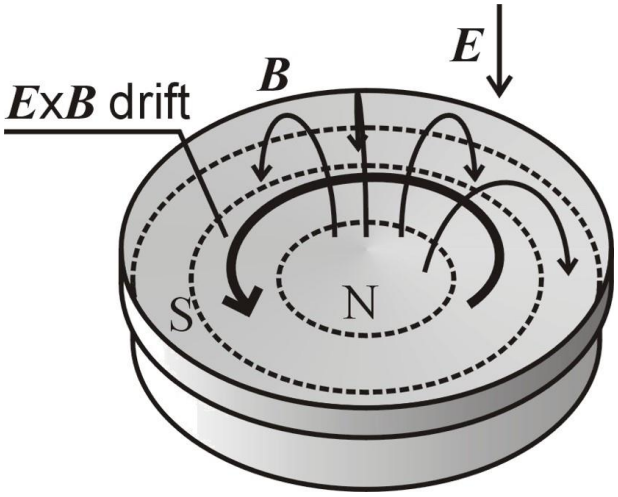

Figure 3.7. The principle of a magnetron
(Source: Vossen 1992)

The created magnetic field constrain the motion of the secondary electron and make them trap in a close region of the target surface. When the electrons are trapped at a close vicinity of the target surface, the probability of an ionization process is largely ascended. The magnetic and electric field interaction creates electron drift path on the surface of sputtering target and it traps large number of electrons (Figure 3.7). This trap causes electrons to collide with an Ar atoms and it increases ionization probabilities. Deposition rate promotes to 10-100 times faster in comparison with sputtering without

magnetron configuration. Ionization efficiency can be provided by less number of argon atoms at a lower pressure in magnetron sputtering. Magnets provide more collisions and great number of ions that make glow discharge easier to form. The easier formation of plasma needs lower power or voltage to be sustained. Another advantage of magnets is that position of the electrons and ions collision path is placed according to sample and it makes uniform and thick deposition on the substrate. This advantage is continued up to erosion in a deep groove in the target face which occur after long time usage, and it bring to non-uniformity film on substrate (Ohring 2001; Böhlmark 2006).

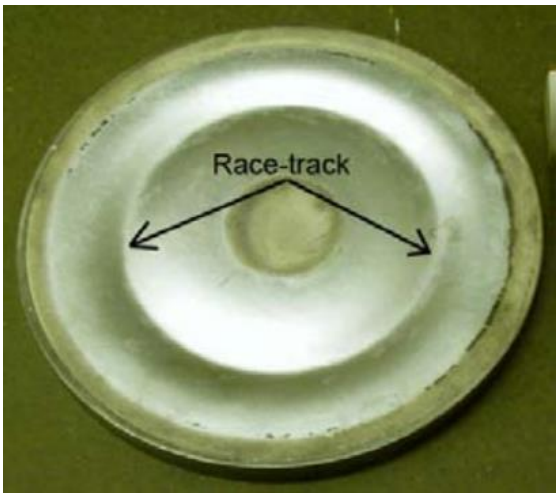

Figure 3.8. Racetrack on target surface
(Source: Böhlmark, 2006)

The drift of the guiding center of the particle is denoted v_{gc}. The velocity of the guiding center can be calculated according to

$$v_{gc} = \frac{ExB}{B^2} \tag{3.11}$$

By the interaction of electric and magnetic field, an electromagnetic force is exerted on electrons and they follow a helical path that is also called the drift path. Ions are also exposed to the same force, but they have larger mass than electrons so that ions drift more per cycle but execute less cycles per second. Electrons and ions are drifted with a cycloidal motion on the target surface and target surface is eroded by this motion a so-called race-track is created (Chen and Smith 1984).

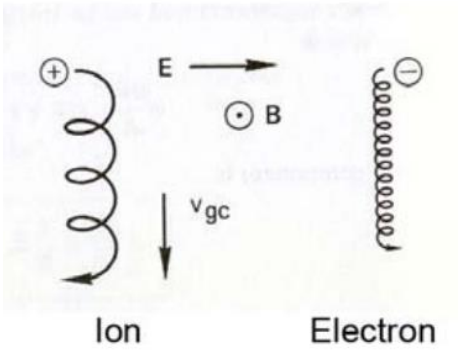

Figure 3.9. Particle drifts in crossed magnetic and electric fields
(Source: Chen and Smith 1984)

3.9.2.2.3. RF

Using the conventional DC method to sputter insulating samples is not efficient because the ion flux is rejected by the positive charge on the target surface and stop the sputtering process. Alternating current can be employed for thin film deposition by insulator target material. In DC sputtering, electric field manipulate energetic ions to the cathode but in RF sputtering, electrodes alternate between each other by applying alternating current. This is what happens at lower frequency such as kHz in RF sputtering but when RF frequency is raised to MHz, the area of electrodes become the important factor to manipulate the ions to substrate. The area of anode (chamber walls) is naturally greater than the area of cathode (target). Target electrode receive less ion density than anode. RF current density must be higher at smaller electrode to provide current continuity. On the other way, electron density is defined by applied potential and it is not depend on electrode surface area. Because the target encounter higher density of electron than ion density, target is applied higher potential than anode and it means that target has negative potential. For this reason, ions manipulation are solely on target electrode. Furthermore, RF cycles creates a capacitive coupling and secondary electrons are easily maintained at cathode region.

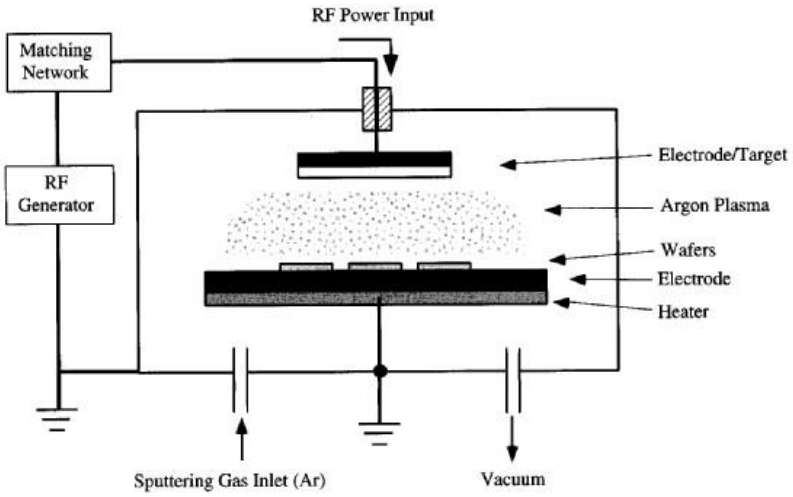

Figure 3.10. RF sputtering
(Source: RF sputtering 2011)

3.9.2.2.4. Reactive Sputtering

A reactive gas such as oxygen is flowed in to vacuum environment beside the inert sputter gas (usually argon). This sputtering method provide functional deposition reacting with target composition and enable to form insulative thin film by using DC sputtering. The nitrides, carbides and other compounds such as sulfites may be deposited in this way by using a suitable reactive gas. Another advantage of reactive sputtering is that deposition in a high purity is much easier than deposition from a specific target with a specific composition. Using a reactive gas in a reactive sputtering enable to control the stoichiometry of the deposited film composition. To control stoichiometry preciously in reactive sputtering is related to how good enough to deal with the control the gas pressure and sputtering rate significantly

A mixture of inert + reactive gases used for sputtering:

Oxides – Al_2O_3, SiO_2, Ta_2O_5 (O_2 mixed with Ar)

Nitrides – TaN, TiN, Si_3N_4 (N_2, NH_3, mixed with Ar)

Carbides – TiC, WC, SiC (CH_4, C_2H_4, C_3H_8, mixed with Ar)

3.9.2.2.5. Ionized Physical Vapor Deposition (I-PVD)

In conventional magnetron sputtering, the majority of the ions is from a reactive gas or an inert gas which is enforced to collided to sputtering target and remove sputtering atom from the surface. The ionized sputtering atom is about 1 % fraction of sputtering material. In this method, sputtering atoms are ionized and accelerated to the substrate. An RF coil is rounded the plasma to trigger the collisions and then to create the ions. By this method, it is possible to reach 50-80 % atom ionized of sputtering material. Most sputtered atoms can reach on substrates with complex shapes and it is a better solution than a collimator sputtering in this way. Because it provides a narrow distribution of arrival angles, which may be useful when filling or coating the bottom of deep contact hole (Monica MC, et al. 2000).

3.9.2.2.6. Ion Beam Sputtering Deposition (IBSD)

IBSD system include multicomponent or multilayered materials using a multi-target mounted to ion gun scheme. Desired target is fronted to ion gun by rotating target wheel. IBSD is a feasible system for formation of multilayer thin films and eaiser to sustain several coating in-situ. Lower pressure is needed sputter deposition (10^{-4} Torr). In this method, adhesion of samples are enhanced and micro-structure of the film is efficiently controlled. System yields excellent coverage at small thicknesses and on high aspect ratio features. The system is equipped with many elements as shown in Figure 3.11 that brings many parameters to user to engineer film for desired properties (Mcguire, et al. 1999).

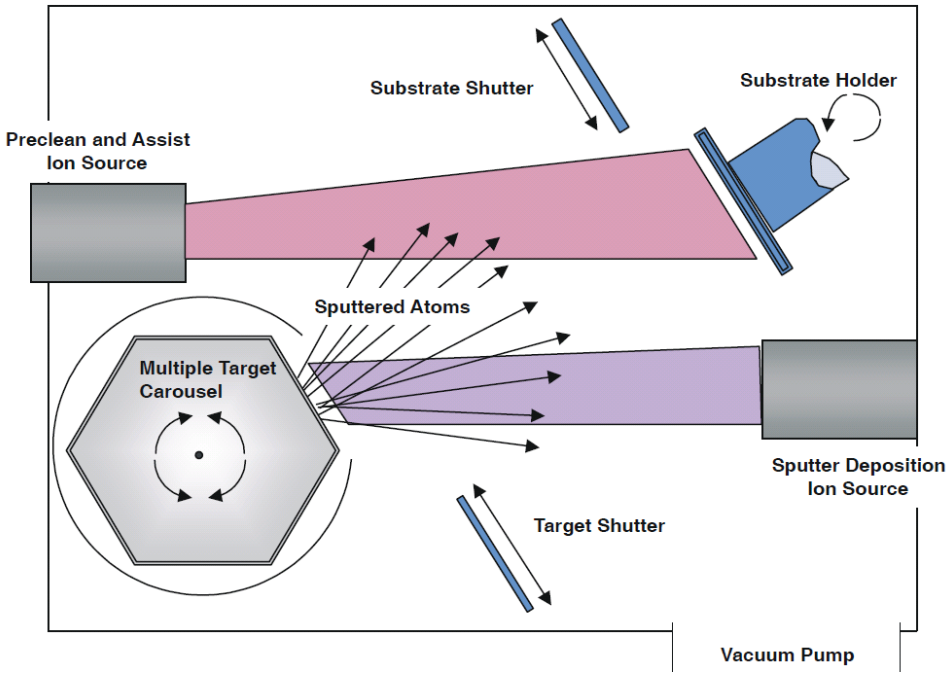

Figure 3.11. Ion Beam Sputtering Deposition (IBSD) System

3.9.2.2.7. Inverted Cylindrical Magnetron

In thin film technology, there are various shapes of samples. An inverted cylindrical magnetron (ICM) device for a continuous all-side deposition onto cylindrical samples such as wires or synthetic fibers is designed. Amberg et al. determined that all-side of fibers and wires can be deposited homogenously and ICM can be employed for a continuous deposition of metal films. (Amberg, et al. 2004). This system is good for continuous system such as roll to roll system and used sample can be in a complex geometry. Image that the internal surface of a pipe should be sputter. Then, this pipe should surrender the target as shown in Figure 3.12-a (Andersson and Anders 2013). But if you have a fiber to coat, target should surrender the fiber as shown in Figure 3.12-b.

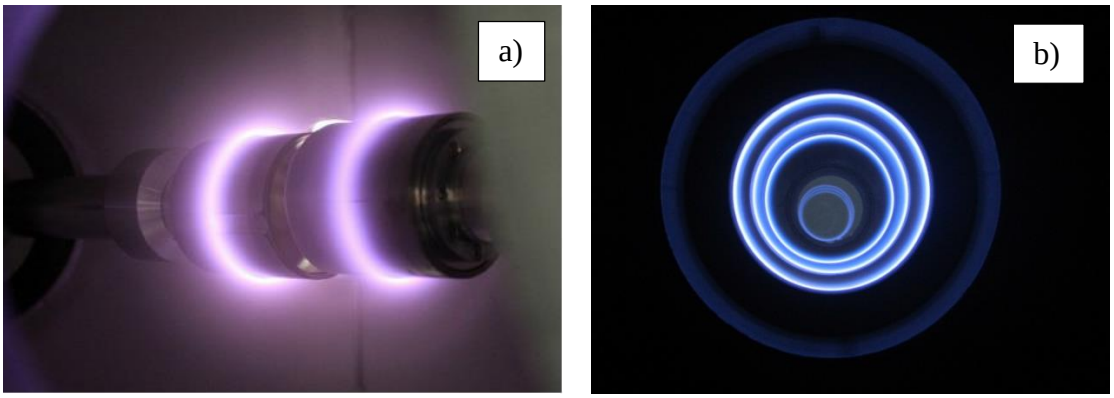

Figure 3.12. a, b; Inverted Cylindrical Magnetron Sputtering Systems
(Source: Dual HIPIMS 2014)

The electrical and magnetic line combination of our inverted cylindrical magnetron sputtering system shown as in figure from side view. Target materials have race-track at the center of surface of the cylindrical target. Because drift velocity line follow this path due to ExB combination or direction. Due to the combination, cylindrical shaped plasma will be obtained so ejected target atom will go towards the center of cylinder where our fiber exist. Due to the combination, this system work perfectly and homogeneously to coat cylindrical samples such as fibers.

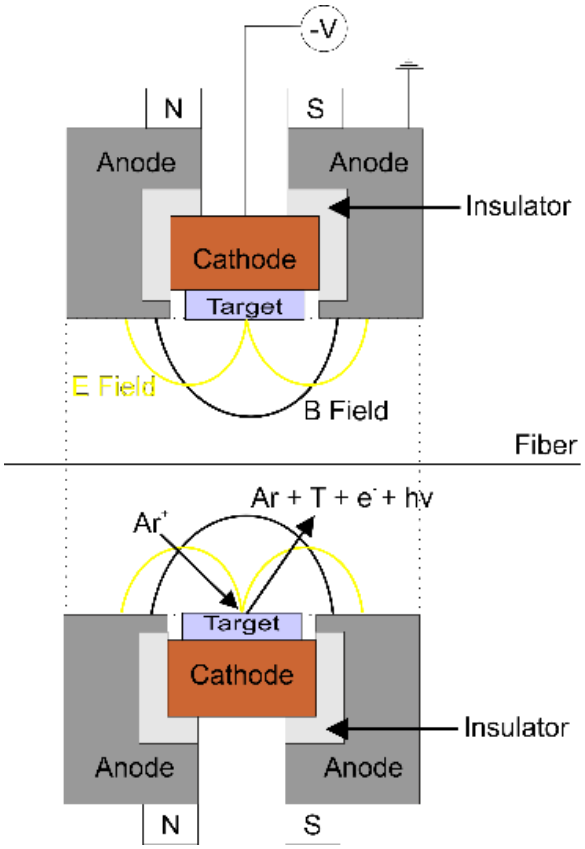

Figure 3.13. Working principle of ring shaped target

3.10. Electrical Conduction Process in Thin Films

All metals have metallic bond and electrons can freely move among the metallic atoms. It can be described as electron cloud and these electrons are not belong to any specific atom. Conduction in metals is provided via these electron and because all electrons are free and mobile, metals are very good electric conductor. Good crystallite is also an advantage of being good conductor for metals. However, there are some imperfections that bring some constraints to conduct well which are vibrating atoms, crystal defect and impurities. The quantization of atomic vibration is called phonon and phonons and mostly conduction electrons are responsible for thermal conduction in metal.

The growth process of thin film is explained before. The imperfections that I mention above can occur in thin film growth step and it depends on vacuum levels, sample surface adhesion, applied power, impinging target atoms energy, and so on. Furthermore, how imperfections effect the conductivity in metallic thin film can be explained by the

equation below which is called Mathieson's rule. This rule state on two assumptions which are impurity and phonon scattering are independent and the relaxation time is isotopic. It is concluded that resistivity of a metal is obtained by adding the thermal, impurity and defect resistivity's. Electron collisions with phonon, impurities and defects can cause the scattering of them elastically or inelastically. Impurities and defects act as scattering centers which increase numbers of electron-scattering and increase enhancement of resistivity (Callister and Rethwisch 2007).

$$\rho = \rho_{Th} + \rho_I + \rho_D \tag{3.11}$$

3.10.1. Scattering Mechanism in Thin Films

It is important to understand the scattering mechanism of the electron affecting the conductivity in thin film. Electron conduction is proceeded by collisions with phonons or scattering at room temperature and above. The factors affecting resistivity of thin metallic film can be ordered such as isotropic (intrinsic) electron scattering, surface scatterings, grain-boundary scattering.

There are many studies about this mechanism in the literature. Wei Luo and Xiaojing Zheng concluded that when the thickness is of the order of the mean free path, the external surfaces scattering is the main factor. This result is helpful to study the thermal properties of nano-materials and design new devices in the future. On the other hand, the surfaces and grain boundaries scattering are the dominant processes to metallic thin films (Luo and Zhang 2010)

Grain size and surface roughness becomes significant that effect conduction in thin film, when mean free path and thin film thickness are nearly same. When the grain size of nanocrystalline metallic films is either comparable to or less than the electron mean free path, the grain boundary and surface scatter electrons strongly. The energy of scattered electrons can be partly transferred across the grain boundary via electron-phonon scattering because phonons can transport through the grain boundary more readily than electrons. This results in the evidently reduced electrical conductivity and less reduced thermal conductivity.

It can be concluded that if thin film thickness is less than the electron mean free path, electron scatter and resistance would be measured higher. Scattering simulates the materials intrinsic result diminishes and measured resistivity is higher than materials original resistivity.

CHAPTER 4

EXPERIMENTAL PROCEDURES

4.1. Deposition Materials

4.1.1. Silver

Silver is used in this thesis because of its good conductivity and antimicrobial property. Silver was metalized on insulator fibers to promote them conductor. Conductor and antibacterial fibers were aimed to be woven into fabrics in order to obtain antistatic textile.

Silver, is grey, shining and precious metal and it has been widely used in daily life. Its chemical symbol is Ag coming from Greek word "Argentum" and it has 47 atomic number (Chen and Schluesener 2008). Silver has good ductility and highest electrical and thermal conductivity among all metals, besides, it has low contact resistance. Silver has FCC crystal structure which has highest atomic package density among other structure types. This property can give clue about its high conductivity because more atoms on lattice means more electron to be mobile to participate conduction. Table 4.1 shows some other properties of silver.

Table 4.1. Properties of silver

Bulk resistivity (μΩ.cm) at 20 ^{o}C	1.59
Mean free path of electron (nm)	52
Thermal conductivity (W/cm.K)	4.25
Melting point (^{o}C)	961

Silver has been highly commercialized due to its highly desirable properties and applications in various industries. Silver is used in water purification, solar energy,

mirrors reflectants, coating, silverware, jewelry, photography, coins, printed circuitry, and chemical catalyst, electrical, pharmaceuticals, dentistry and clothing (www.silverinstitute.org). I will focus on its usage in textile and medical applications.

4.1.1.1. Silver in Biomedical

Silver is attracting owing to its wide range of research and application in biomedical, food industry. Even in ancient times, silver is believed to treat of ulcers and this anti-disease properties was claimed by, father of modern medicine "Hippocrates". The participation of silver to medical applications cannot be underestimated. In daily life, consumers may have nanosilver containing room spays, laundry detergents, water purificants and wall paint (Chaloupka et al. 2010: Bosetti et al. 2002). Drake and Hazel wood have reviewed health effects of silver and silver compounds from a perspective of occupational exposure. Metallic silver was viewed to be a minimal health risk (Drake and Hazelwood, 2005). In addition, NS has been integrated into various food contact materials, such as plastics used to fabricate food containers, refrigerator surfaces, storage bags and chopping boards, under the pretext of preserving foods longer by inhibiting microorganism growth (Sekhon, 2010).

4.1.1.2. Silver in Textiles

Silver is clearly the most commonly used elements for inorganic coating for textile products. Silver nanoparticles are also incorporated into textiles for manufacture of clothing, underwear and socks (Vigneshwaran et al., 2007). Clothing manufacturers have incorporated nanosilver into fabrics for socks and exploit the antibacterial activity for neutralization of odor-forming bacteria (Benn and Westerhoff, 2008,). Silver has antibacterial property and also exhibit low toxicity towards mammalian cells (Scholz, 2005).

4.1.2. Polymers

Plastic is one of the most commercial and widespread materials in our life. Most plastics are good electrical insulator, tending to acquire a strong electrostatic charge which may cause trouble and malfunction in the operation of the electric devices, and are dangerous of being flamed (Bajaj, 2000: Hausmann, 2007). Polymers are separated into two groups which are thermosets and thermoplastics. Thermosets include the cross-link entanglement and irreversible chemical bonds is formed during curing process. They are heat resistant and strength polymers. On the other hand, thermoplastics can be re-shaped by applying heat and there occurs reversible chemical bond. Thermoplastics can be re-molded and re-cycled. It is easier to bend them which is desirable for many polymer applications. The properties of the polymers is determined by number and sort of its repeating units and structure, formation mechanism and applied additives during production (Brydson 1999).

There are several examples of polymers such as, Polyamide (PA), Polyethylene (PE), Polytetrafluoroethylene (PTFE), Polypropylene (PP), and Polyethylene terephthalate (PET) and these examples are the most popular polymer using in research and industry.

4.1.2.1. History of Polymers

First official examples of polymer is showed in 1830 and it was a semi-synthetic polymer produced by Henri Braconnot. But polymer term is bounced up by Jons Jakob Berzelius in 1833. However, rubber was employed long time ago before these researches in polymers. This time interval can be called the realization of a new material group.

The birth of a plastic technology is followed after this term and remarkable inventions brought an enthusiasm and focus in polymer industry. While Herman Mark remained agnostic on the topic of Hermann Staudinger's macromolecules, by 1928, when he was working for I.G. Farben, he had become a believer in polymers after seeing his own x-ray crystallography work on the structure of cellulose. Hermann's works were revealing the nature of polymers and he was awarded the Nobel Prize in 1953.

The World War II made an increase in demand of new type of polymers and silk, nylon, synthetic rubber and teflon are invented to encounter this necessities. Plastics are used as substitute materials in that term and polymer industry was grown strongly. The "Plastics" age was dominant at 1950-1970 years so that, polymer science encouraged people to establish institutes and form the societies resulting in many researches. Polystyrene, polyvinylchloride, low density polyethylene, glass-fiber reinforced polyesters, epoxy resins and aliphatic polyamides were generated in this time interval (Fruton 2002).

Engineering in polymers is still in development which originates from 1970. New polymers development gathers important improvement and it is focused to proceed parallel demand of nanotechnology and thin film technology. Polymer industry is strongly desirable because modern technology needs smart, safe, small, durable and flexible materials (Sizing and Dekker 2013)

4.1.2.2. Polyamide

Polyamide (PA) as known nylon6 or nylon66 is used in this thesis as substrate to deposit silver thin film on. According to literature, it is difficult to deposit a metallic thin film on a polymeric surface and it is partially proved by our experiences. PA fiber is chosen as sample to deposit silver thin film because silver thin film has better adhesion property on PA fiber surface when compared with polypropylene, PET and polyethylene.

Polyamides are in the family of synthetic and semi-crystaltalline polymers. They are electrically insulator and there are two kind of polyamide which are PA6 and PA66. 6 and 66 represent number of carbon atom including in repeating unit. They have good surface adhesion property and high and medium mechanical strength. PA has good fatigue strength, very good wear resistance and good sliding properties. Polyamide is chemical resist but easy to process. Some properties of polyamide is demonstrated in Table 4.2.

Table 4.2. Properties of polyamide

Tensile Strength N/mm²	90 - 185
Thermal Coefficient of expansion	90 - 20/70 x 10-6
Max Cont. Use Temp. ºC	150 - 185
Density g/cm^3	1.13 - 1.35/1.41

Polyamides have wide range of application in polymer industry. PA is an engineering plastic and used in automobile, construction, pipe technology, oil and gas components, and electrical application. It is dominant polymer in our life and many of its applications can be released around.

4.2. Experimental Set-up

4.2.1. Design

In conventional magnetron sputtering system, substrates are planar and flat, so sputtering cathode and target are planar. Cathode is suitable to growth thin film on just one part of substrate which is faced to sputtering target. Some sputtering systems have dual or triple target which is positioned around the sample to deposit more side of substrate. Although a cylindrical substrate is surrounded equally all sides by four target around, sample would not coated homogenously. It is obvious that planar magnetron sputtering is not convenient to coat cylindrical substrates such as fibers.

In this thesis, silver thin film was aimed to deposit on fiber surface. In our design, the number of ring shaped targets were purposed to enhance the sputtering rate at high speed. New targets were designed with greater diameter than our previous study (Meric 2011). This increase in target diameter would allow fibers to cycle more and this would enable greater deposition rate. In our previous study, fibers only could reach 15 cycles but now they are 35 cycles. This design offers to employ four 99.99% pure silver targets according to these criteria. More fibers cycling through the targets and increase in number of targets bring the opportunity of increase in fibers speed during sputtering.

Figure 4.1. Our inverted cylindrical magnetron sputtering system

Roll to roll mechanism was also added to our inverted cylindrical magnetron (ICM) sputtering system. Our ICM roughly include two vacuum chambers and sputtering targets which take place between these vacuum chamber and they are all connected. In one vacuum chamber, there is a feeding roll which enables to send fibers through targets to winding ling roll which is positioned in other vacuum chamber. A rotator machine is used to rotate the winding roll and it is integrated to vacuum chamber by magnetic coupling. The speed of rotator machine can arrangeable by a controller and speed is constant at arranged value. Another machine is mounted to vacuum chamber in order to provide winding roll to wind homogeneously.

4.2.2. System Calibration and Optimization

Sputtering system was redesigned according to our previous sputtering system and number of targets, change in diameter of targets. Our new ICM sputtering system was needed calibration and optimization to determine the distance between substrate and target surface in order to achieve the most efficient sputtering distance. A glass lamella is

used as a sample instead of polymer fiber so that silver thin film could be deposited on it. Here, the distance between substrate and target surface were changed by 1 cm apart for every time. Sample positioning was started from the ring shaped target center and distance get close to target surface by 1 every time. The thickness of the silver thin film on the glass lamella was measured by a surface profilometer to find the most efficient position of the sample in our system.

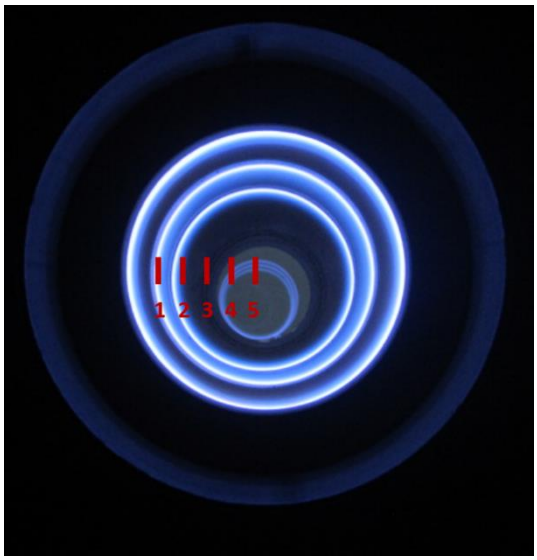

Figure 4.2. ICM system calibration to find efficient staget to substrate distance

In additions many calibrations were done for winding roll speed and minimum and maximum amount of gas flow. Several measurements were proceeded to detect vacuum level in order to make sure if there is a vacuum leak. Cooling system was also required many tests for water leak in targets. Many trial of applied power to targets were tried to find minimum and maximum values of power correspond to flowed gas value.

4.2.3. Operation

In this research, two targets were employed in our ICM sputtering system. After evacuated the chamber by a rough pomp to low vacuum which is about 10^{-2} torr, a turbo molecular pomp was employed up to 10^{-5} torr vacuum level. Ar gas was flowed into the chamber using mass flow controller. PA fibers were used as substrates and fibers roll was

positioned in first vacuum chamber. Fibers were sent to winding roll and they were making 35 cycles while sputtering was proceeding. Power applied to each silver targets for the formation of plasma in the vacuum chamber by DC power supplies. Thickness of thin film and electrical characterization are studied according to various fibers speed at constant power and current but at different gas flow values.

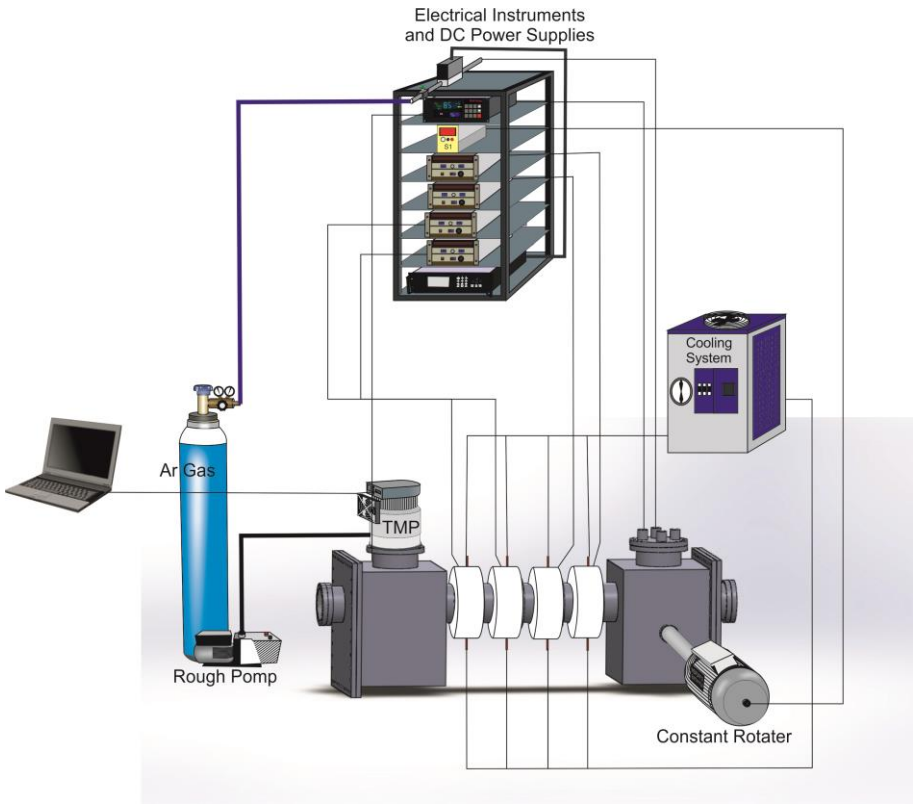

Figure 4.3. Experimental set-up of our ICM system

4.2.4. Studied Parameters

PA fibers whose diameters are 85 and 150 um were deposited silver thin film. These fibers were tried at various fiber speed during deposition which are 20 m/min to 80m/min with increment 5 m/min. Power was constant at 140 Watt for all targets. Obtained fibers resistance deals with silver thin film thickness on them. Fibers resistance, thin film thickness and fiber speed were calibrated. Additional factor is amount of gas flow so that all of parameter re-calibrated according to second gas flow value.

4.3. Characterization Procedures

4.3.1. Optical Microscopy Studies

The optical microscopy is widely used in life science as well as materials science to magnify the images of the small samples. Photons are generally used in the range of visible light for picturing. There are several types of optical microscopy which deals with the resolution of sample even they have very complex structure. Compound, Stereo and Confocal Laser Scanning are some of them. Mainly set of lenses is used to enlarge the images and each lenses have different magnification and contrast.

Optical imaging of silver coated PA fibers were investigated in order to observe the roughness and homogeneity of surface of thin film. For this purpose, a Nikon Optical Microscope with Image Capture was employed at clean room in physics department at IZTECH.

4.3.2. Scanning Electron Microscope (SEM) Studies

SEM uses a focused beam of high-energy electrons to generate a variety of signals at the surface of solid specimens. Working principle of SEM is attributed to signals coming from secondary electrons that produce images of surface of the material. Backscattered electrons (BSE), and diffracted backscattered electrons (BSED) are used to determine crystal structures and orientations of minerals. X-rays, visible light and heat are used for elemental analysis as continuum sources. In summary, SEM is used to investigate the microstructural and morphological structure of materials by yielding high resolution imaging of materials surface besides elemental analysis that materials include.

In this research, Scanning Electron Microscopy (SEM) and Energy-Dispersive X-Ray (EDX) elemental analysis were employed on silver coated and uncoated fiber surfaces. For this purpose, Quanta 250FEG scanning electron microscope at IZTECH Materials Research Center was performed.

4.3.3. XRD Studies

The concept of XRD (X-Ray Diffraction) is significantly used to determine the surface structural characterization and also crystal plane orientation. This technique is based on the diffraction of X-Ray waves by a crystal lattice. Principally, the wavelength of the wave is in the range of the lattice constants that provides to take signals from diffracted lights to probe the crystal structure of material.

XRD analysis were examined to identify crystal structure of silver coated and uncoated PA fiber. The crystal structures of fabricated silver thin films on PA fiber were analyzed by X-ray diffractometry (XRD). The XRD was performed in the Bragg-Brentano focusing geometry from 5º to 80° on a Phillips X'Pert Pro X-Ray diffractometry at IZTECH Materials Research Center.

4.3.4. Electrical Results

Resistance of silver coated polymer fibers were measured by analog or digital multimeter or same called it ohmmeter. Materials are allowed conductivity by their resistance and resistance can be expressed by ohm's law.

OHM's Law:

$$V = I.R \tag{4.1}$$

The equation determines that applied voltage (V) and measured current (I) is proportional to each other and it is constant by resistance (R) for same size of same material. A standard multimeter inject a known voltage into the target material so that it can measure the current and then calculate the resistance. There are two indicators that affects the resistance. First one is what material is made of and the second one is the geometry of the material. The relation between resistance and resistivity can be revealed by bulk resistivity formula.

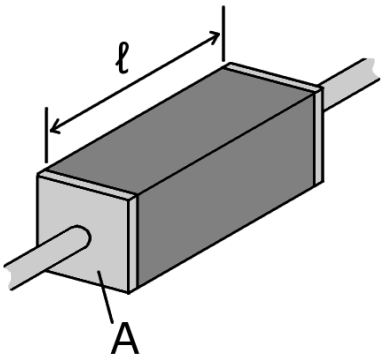

Figure 4.4. Illustration of cross-section area and length of bulk resistivity
(Source: Resistivity in materials, 2015)

$$R = \rho \frac{l}{A} \tag{4.2}$$

Where l is the length of the conductor, measured in centimeters [cm], A is the cross-section area of the conductor measured in square centimeters [cm²] and ρ is the resistivity measured in Ω.cm. Resistivity is material specific resistance and it does not change but resistance can change. Resistivity inverse proportional with conductivity and it gives material ability to resist the electric current.

4.3.5. Thin Film Thickness Measurements

It is not easy to measure the thin film thickness on cylindrical sample comparing to flat samples. A surface profilometer which is convenient for planar samples can't be employed cylindrical samples. Three methods were followed to obtain thin film thickness on a fiber. Three of them were used to obtain the thickness virtually and results were compared as following.

4.3.5.1. Calculating from Measured Resistance

The silver theoretical resistivity is known and bulk resistivity formula can help us to obtain the thickness by measuring the resistance of silver coated fiber in 1 cm interval. The initial diameter of the polymer fiber was known before sputtering. Cross-section area can be calculated by the formula which is

$$R = \rho \frac{l}{A} \tag{4.3}$$

$$A = 2\pi rt \tag{4.4}$$

Where t is the thin film thickness and r is the initial radius of fiber before coating. All known parameter can be put into bulk resistivity formula and unknown parameter can be solved which is thin film thickness.

4.3.5.2. Calculating from Deposited Silver Mass

Another option to calculate silver thin film thickness by deposited silver mass. Silver density is known and density formula can be driven. Weight of the 10 meter long fiber can be measured before and after the deposition. Difference of the weight can help us to obtain the thickness by using the density formula. Mathematical process can be driven as following;

$$\rho = \frac{M}{V} = \frac{\Delta M}{2\pi rtl} \Rightarrow t = \frac{\Delta M}{2\pi rl\rho} \tag{4.5}$$

Where ρ = 10.49 g·cm^{-3}, l = 1000 cm, r= 0.00750 and 0.00425 cm. Delta M is just represent the deposited silver.

Figure 4.5. A schematic sketch of the silver thin film on PA fiber

4.3.5.3. Calculating from Calibration Sample

A glass lamella were used as a sample instead of polymer fiber so that silver thin film could be deposited on it by using our inverted cylindrical magnetron sputtering with same parameters. Glass lamella is planer shaped so that a surface profilometer was used to obtain the thickness.

4.3.6. Antistatic Tests

TS EN 1149 test standard was performed to analysis the surface electrical resistance of the fabrics. There are two co-centric rings operating as two electrodes. Sample is placed as contact between electrodes. A high voltage is applied to outer electrode while inner one in sensing mode. The surface resistance is basically a function of the ratio between the inner diameter of the outer electrode and the outer diameter of the inner electrode; the volume resistance is basically a function of the area of the inner electrode and the thickness of the test specimen.

Figure 4.6. Surface resistance measurement test probe

Silver coated polymer fiber can be woven into a fabric with 10 mm interval horizontally and vertically. The surface resistance of obtained fabric were measured to define if it is in the range of antistatic property or not. Fabrics were 35 x 35 cm width and length. A surface resistance test probe which working principle matches with TS EN 1149 test standard was used to investigate the surface resistance of fabrics.

Figure 4.7. 35 x 35 cm fabrics woven with 10 mm interval horizontal and vertical

4.3.7. Shielding Tests

Charging of the test specimen is carried out by an induction effect. Immediately under the test specimen, which is horizontally arranged, a field-electrode is positioned, without contacting the specimen. A high voltage is rapidly applied to the field-electrode. If the specimen is conductive, or contains conducting elements, charge of opposite polarity to the field-electrode is induced on the specimen. Field from the field-electrode which impinges on the conducting elements does not pass through the test specimen and the net field is reduced in a way that is characteristic of the material under test. This effect is measured and registered behind the specimen with a suitable field-measuring probe. As the amount of induced charge on the test specimen increases, the net field registered by the measuring probe decreases. It is this decrease in field that is used to determine the half decay time and the shielding factor (TS EN 1149-3).

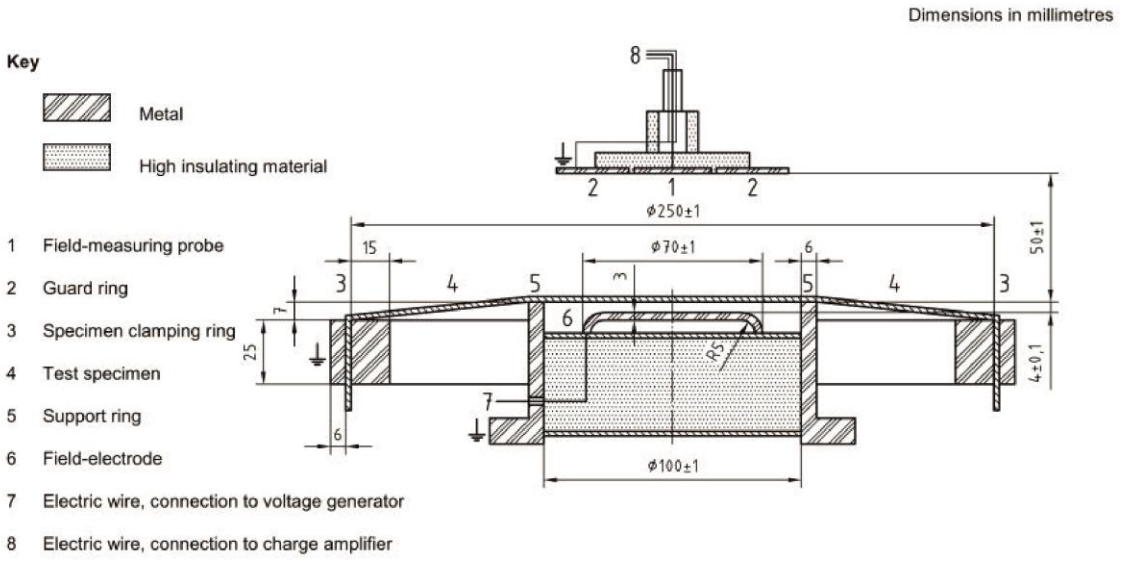

Figure 4.8. Induction charging field-measuring probe
(Source: TS EN 1149-3)

Silver coated polymer fiber can be woven into a fabric with 10 mm interval horizontally and vertically. The surface resistance of obtained fabric were measured to define their shielding property. Fabrics were 35 x 35 cm width and length. These scales

are convenient for our measurement mechanism. An induction charging field-measuring probe was operated to investigate the shielding factor of the fabrics.

4.3.8. Adhesion Tests

The fabrics proceeded in shielding tests and antistatic test were used for adhesion characterization, the values of these test were considered as data of unwashed fabrics .Then, woven fabric were washed in a conventional washing machine then surface resistance and shielding factors were re-measured. Re-test intervals were 10 wash apart each other. Washed fabrics were compared to the previous results and others.

CHAPTER 5

RESULTS AND DISCUSSIONS

5.1. ICM System Optimization

In this analysis, the deposition efficiency was tried to be determined according to distance between deposition substrate and surface of sputtering target. A glass lamella was sent through one target at 0.23 m/min speed and the position of the substrate was brought closer starting from center of target to target surface by 1 cm for every time. Measured thickness revealed that substrate 3.3 cm apart from the target has highest thickness value among other distances. So the substrate should have positioned at this distance. It should be noticed that PA fibers were used as sample in this research and their shape, adhesion and deposition speeds were not same with glass lamella so that the thickness of fiber will be different from 117.5 nm at 3.3 cm far from the target surface. Still, fibers have the highest value of efficiency of deposition at 3.3 cm far from the target surface.

Table 5.1. ICM System calibration data

#	Target to substrate distance (cm)	Thickness of silver on glass sample (nm X 0.23 m/min)
1	1.3	78.5
2	2.3	99.5
3	3.3	117.5
4	4.3	112
5	5.3	93

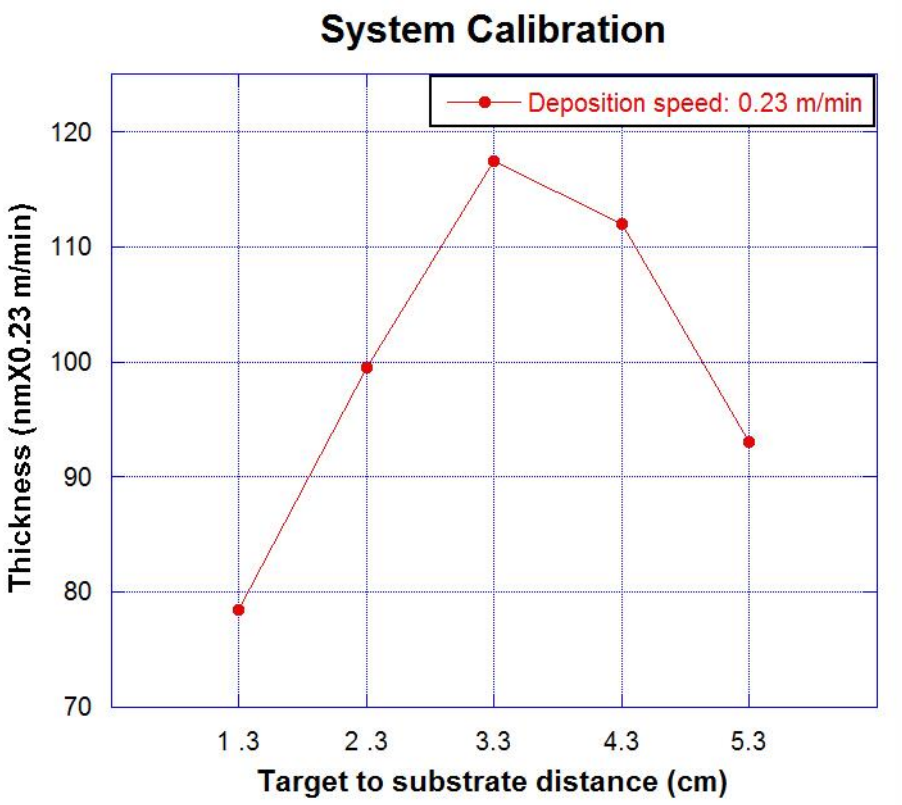

Figure 5.1. The most efficient distance to target surface in ICM system

Deposition rate is proportional to sputtering rate or obtained thickness. Sputtering rate firstly increases by divergent of target from the surface then decreases in the graph. Deposition rate is a function of kinetic energy of sputtering atoms and the kinetic energy of sputtering atoms are affected indirectly by magnetic field lines because these atoms are removed by bombarding ions which are accelerated by same magnetic field (Chen et al. 1999). Ions having grater mass or exerting greater force are exchange large amount of momentum with sputtering atoms which are headed for substrate. Upon this conclusion, magnetic field lines are believed to have their highest radius as 3.3 cm in this ICM system. Sputtering rate increases up to highest magnetic line radius and then decreases.

5.2. Studied Parameters

Several parameters were investigated during silver thin film deposition on PA fibers and the optimum values of them were tried to find when two targets of the system were operated. Deposition speed of fibers were limited 20 m/min to 80 m/min because if fiber speed was slower than 20 m/min, the temperature due to glow discharge was deforming the fibers and tearing apart them. PA fibers were not durable to temperature while deposition speed lower than this speed. PA fibers were not durable to loaded while deposition speed higher than this 80 m/min. That force were made them tore apart. In addition to deposition speed parameter, diameter of fibers and gas flow have different values but number of cycles of the fibers through the plasma, and applied power remained same at 35 cycles and 140 Watt respectively. Diameter of fibers were chosen as 85 um and 150 um. Plasma operation was limited to 80 sccm gas flow because plasma was not sustainable below the 80 sccm gas flow.

Figure 5.2. Silver thin film coated fibers winded on rolls

Table 5.2. Studied parameters

Diameter of fiber (um)	Number of cycles through the plasma	Gas flow (sccm)	Deposition speed (m/min)	Applied power (Watt)
150	35	80	20 to 80	140
150	35	120	20 to 80	140
85	35	80	20 to 80	140
85	35	120	20 to 80	140

5.3. Optical Microscopy Results

Figure 5.2 a shows the optical microscopy image of 150 um in diameter of silver coated PA fiber and figure 5.2 b shows Ag coated PA fiber in 85 um in diameter. Figures show that silver thin film has homogeneously grown on PA fibers. There is no roughness but smooth surface. The result as seen in images satisfy that we have optimum value for coating and thickness of thin film which is aimed previously. Optical microscopy analysis is solely not enough to claim a certain conclusion about materials surface so that SEM analysis were performed because SEM has higher resolution imaging and greater precision of analyzing of morphological structure of surface of a material.

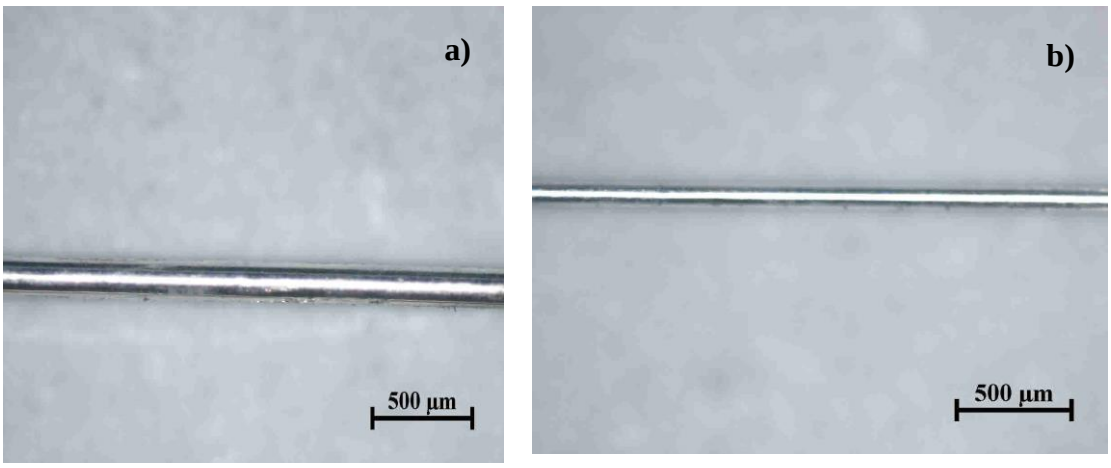

Figure 5.3. Optical microscopy images

5.4. Scanning Electron Microscope (SEM) Studies

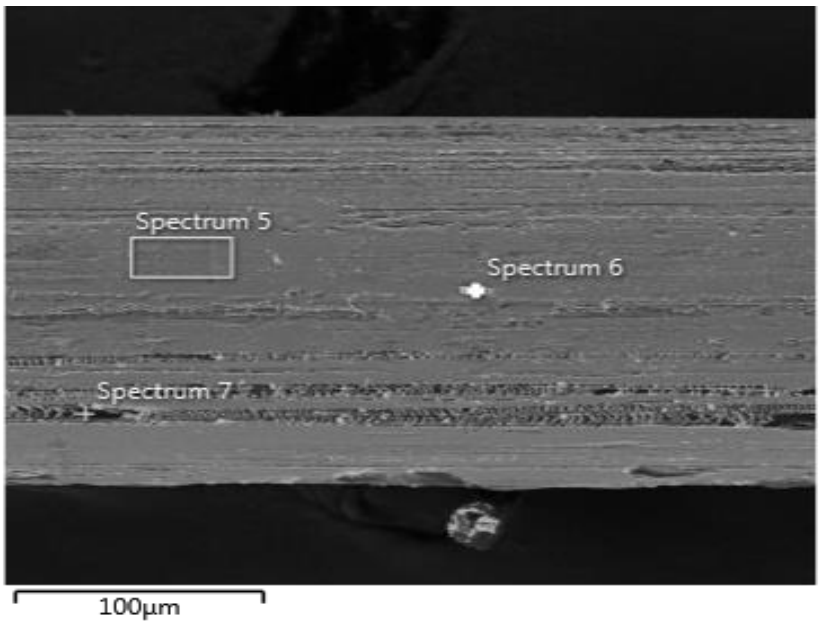

Figure 5.4. SEM image of silver coated fiber

Figure 5.3 represents SEM image of silver coated with 45 m/min deposition speed on monofilament fiber in 150 um diameter at 140 Watt, and 80 sccm gas flow. Scanning electron microscopy analysis proved that silver is coated on all surface of fibers. A few cracks and some roughness were observed. The mechanic deformation is believed to be formed due winding on roll during roll to roll process because silver thin film can easily scratched. Three different region were chosen but the region which represented by spectrum 5 has the common surface morphology.

Table 5.3. EDX analysis of spectrum 5 on silver coated fiber 1

Element	Wt%	Atomic %
C	55.86	66.46
N	22.52	22.97
O	10.13	9.05
Ag	11.49	1.52
Total:	100.00	100.00

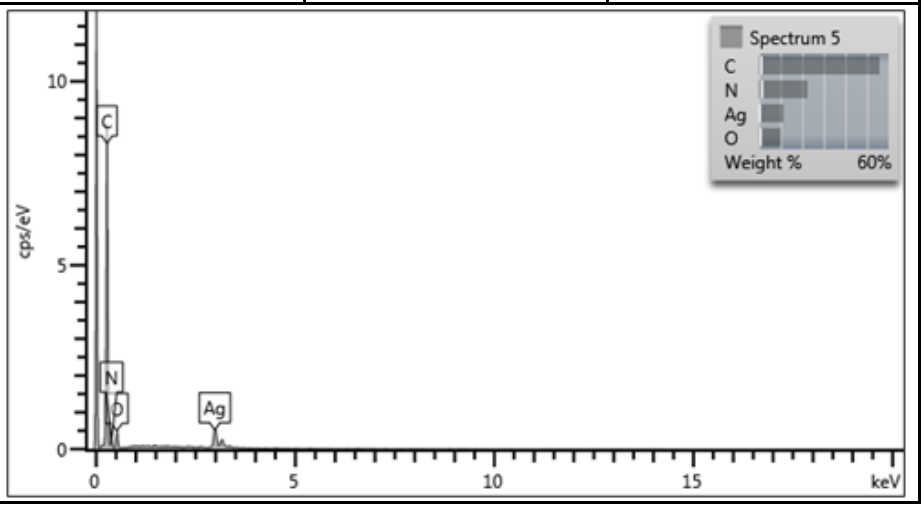

Table 5.4. EDX analysis of spectrum 6 on silver coated fiber 1

Element	Wt%	Atomic %
C	3.00	17.83
N	4.06	20.67
O	0.00	0.00
Ag	92.94	61.50
Total:	100.00	100.00

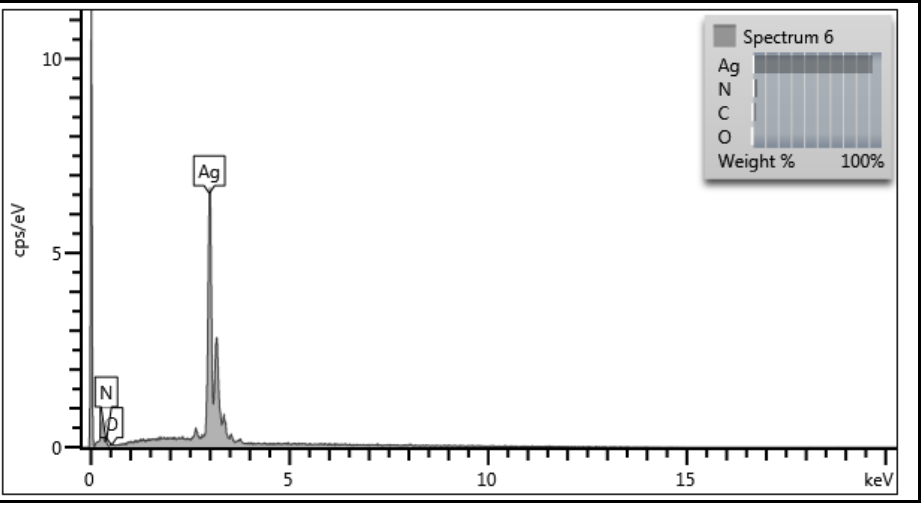

Table 5.5. EDX analysis of spectrum 7 on silver coated fiber 1

Element	Wt%	Atomic %
C	58.65	70.83
N	18.71	19.37
O	8.74	7.93
Ag	13.89	1.87
Total:	100.00	100.00

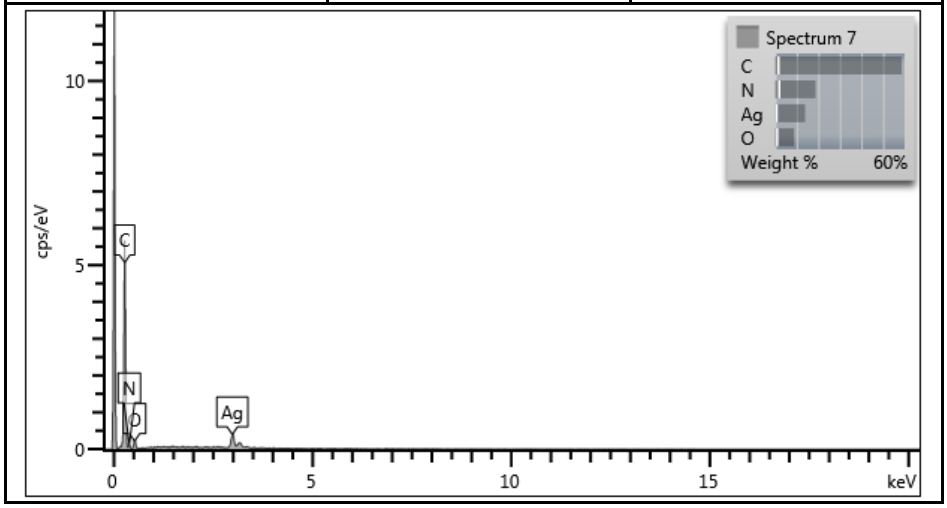

EDX analysis proved that only silver thin film is on the fiber and there is no other impurities or elements. EDX results show carbon, oxygen and nitrogen atom participations. It is because of that EDX uses high energetic ultraviolet light beam and it penetrates to fiber deeply. These participations come from polymeric structure of PA. Spectrum 5 and 7 has almost same EDX analysis and weight and atomic percentages of the elements are nearly same. Spectrum 6 represents a bright point on the fiber surface and it seems that silver has accumulated as that point as proved by EDX analysis.

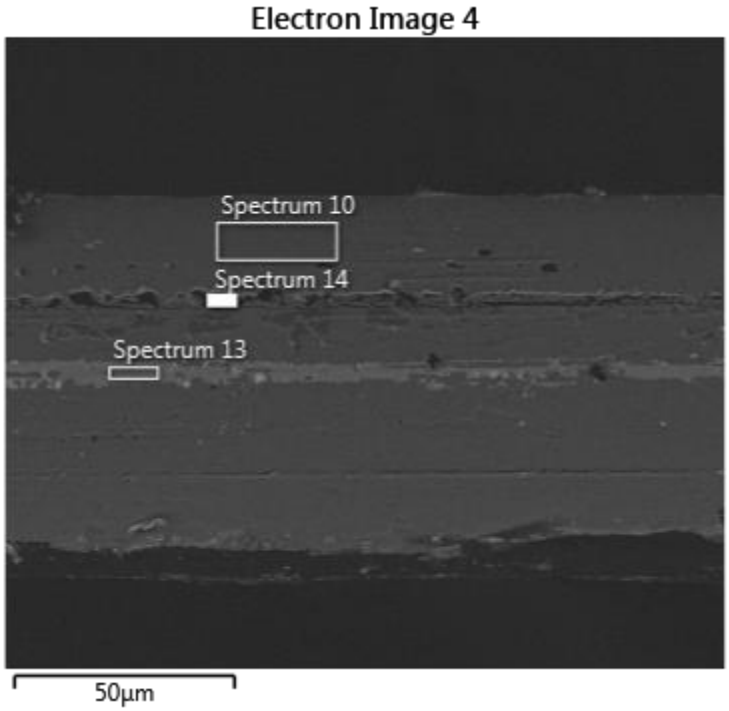

Figure 5.5. SEM image of silver coated fiber 2

Figure 5.5 represents SEM image of silver coated with 20 m/min deposition speed on monofilament fiber in 85 um diameter at 140 Watt, and 80 sccm gas flow. Scanning electron microscopy analysis proved that silver is coated on all surface of fibers. More cracks and more roughness were observed according to fiber in 150 um diameter. These differences can be attributed to the growth mechanism of thin film, because 85 um diametric fiber has less surface area and greater curvature than the fiber in 150 um diameter. So, island growth mechanism is difficult to be formed and less efficient for 85 um diametric fiber. Three different region were chosen but the region which represented by spectrum 10 has the common surface appearance.

Table 5.6. EDX analysis of spectrum 10 on silver coated fiber 2

Element	Wt%	Atomic %
C	44.59	59.32
N	23.04	26.29
O	11.29	11.27
Ag	21.08	3.12
Total:	100.00	100.00

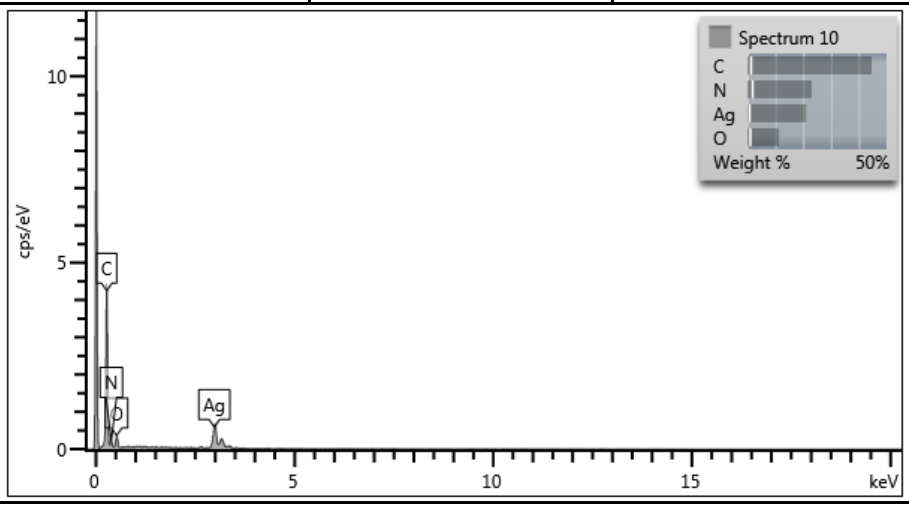

Table 5.7. EDX analysis of spectrum 13 on silver coated fiber 2

Element	Wt%	Atomic %
C	37.69	63.64
N	17.53	25.38
O	2.37	3.01
Ag	42.41	7.97
Total:	100.00	100.00

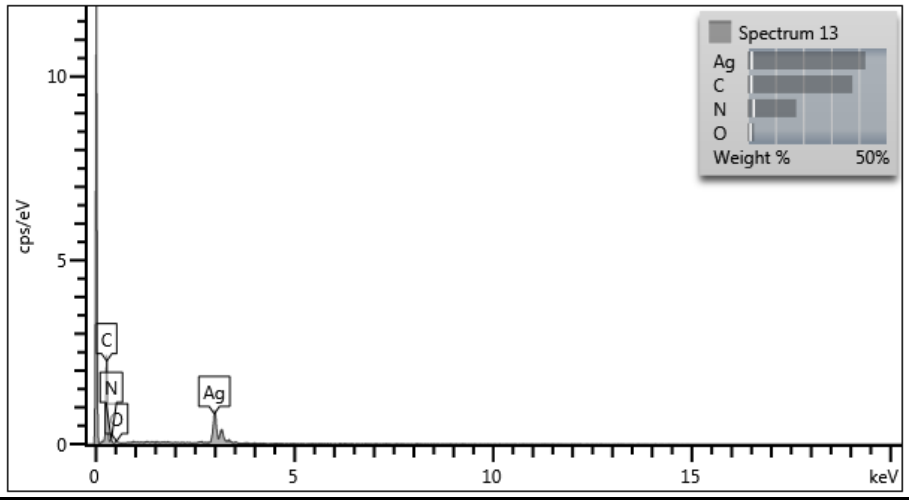

Table 5.8. EDX analysis of spectrum 14 on silver coated fiber 2

Element	Wt%	Atomic %
C	59.17	65.35
N	22.87	21.66
O	15.27	12.66
Ag	2.69	0.33
Total:	100.00	100.00

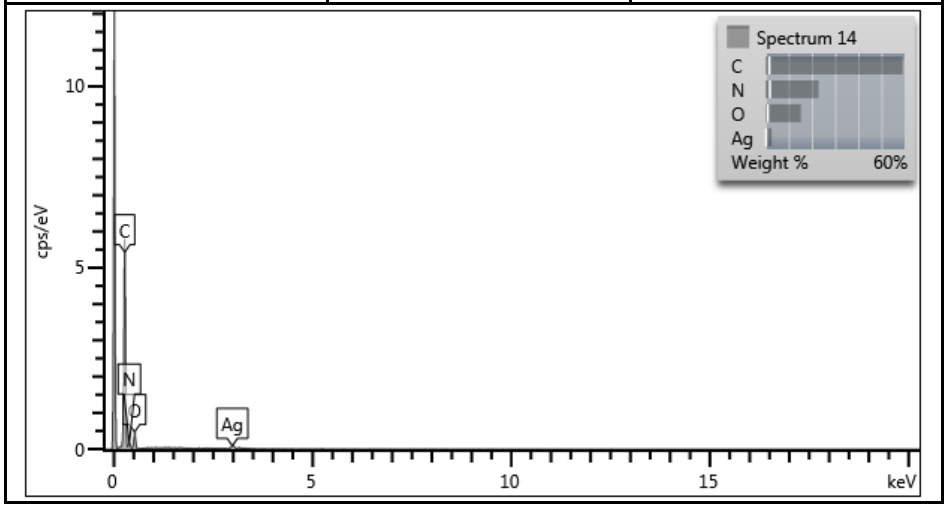

85 um diametric fibers EDX analysis proved again that only silver thin film is on the fiber and there is no other impurities or elements as same analysis for 150 um diametric fiber. There is no exact similarity or very close value of EDX analysis of 85 and 150 um diametric fibers.

5.5. XRD Results

XRD profile was observed from paper of Yeon S. Jung (2004). Jung varied sputtering parameters to observe the change of morphology of silver thin film which were deposited on non-alkali glasses. Two peaks of (111) and (200) planes were observed at that research as shown in Figure.5.6.

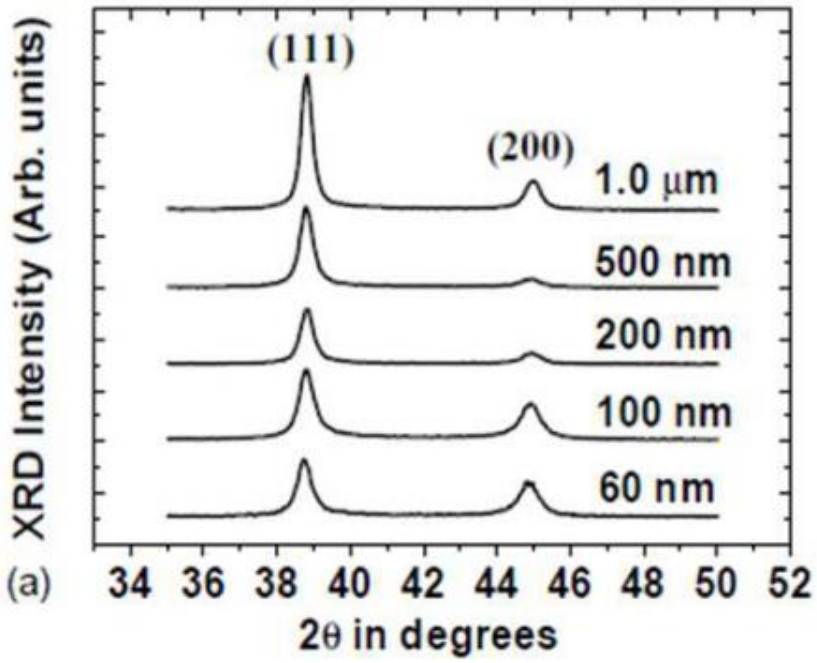

Figure 5.6. X-ray diffraction results from literature
(Jung, 2004)

XRD diffraction patterns show both PA and silver thin film peaks. Blue data show silver coated PA and red one is only PA as shown in Figure 5.7. When the data is compared, (111) and (200) peaks were obtained clearly in silver coated fiber. The crystallization was detected in (111) and (200) planes. Silver was deposited on glass substrate in Jung research but it was deposited on polymer fiber in this research, so that the differences in XRD plots is due to the differences in substrates.

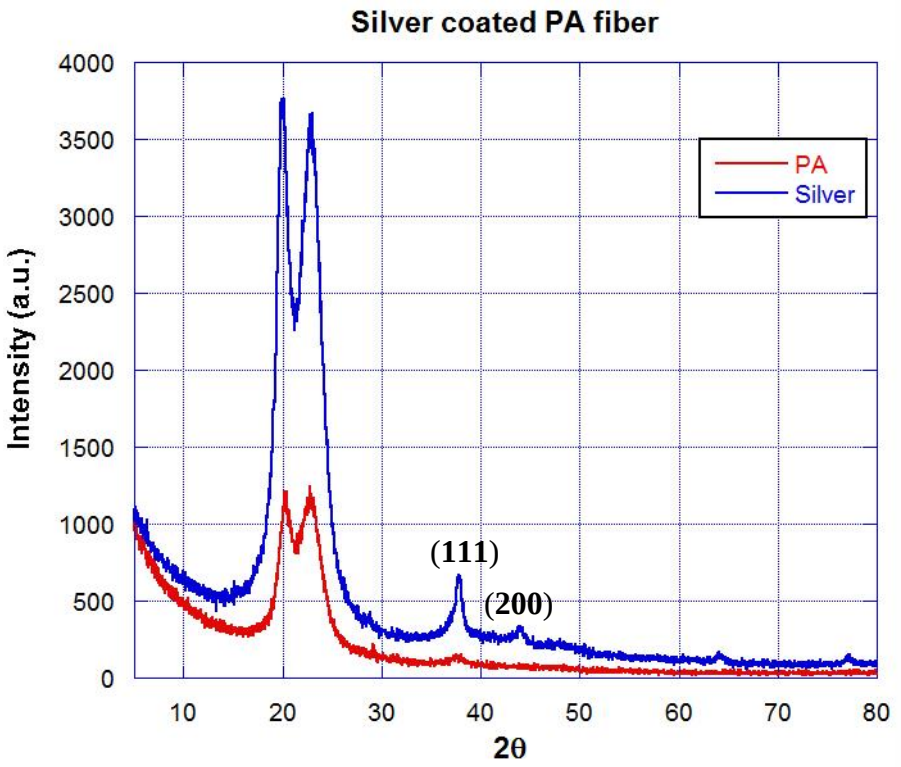

Figure 5.7. XRD graph of uncoated PA and silver coated PA.

5.6. Electrical Results

Resistance and deposition speed relationship were analyzed by measuring resistance of each coated fiber which deposition speed was already known. The thickness of thin film grown on the PA fiber determine the electrical characterization of it. Better crystalline and better homogeneity provide beter electrical conduction. Beside, the much thin fillm growth on PA fiber means less resistance because silver thin film is thicker. For electrical analysis of silver coated fiber with 150 um diameter, Table 5-9 shows row data and Figure 5.8 shows the graph of these data. For electrical analysis of silver coated fiber with 85 um diameter, Table 5-10 shows row data and Figure 5.9 shows the graph of these data.

Table 5.9. Electrical characterization data of silver coated fiber with 150 um diameter

d=150 um	120 sccm	80 sccm
m/min	R(Ω/cm)	R(Ω/cm)
30	26	36
35	42	64
40	60	93
45	71	102
50	78	107
55	97	112
60	131	169
80	253	NA

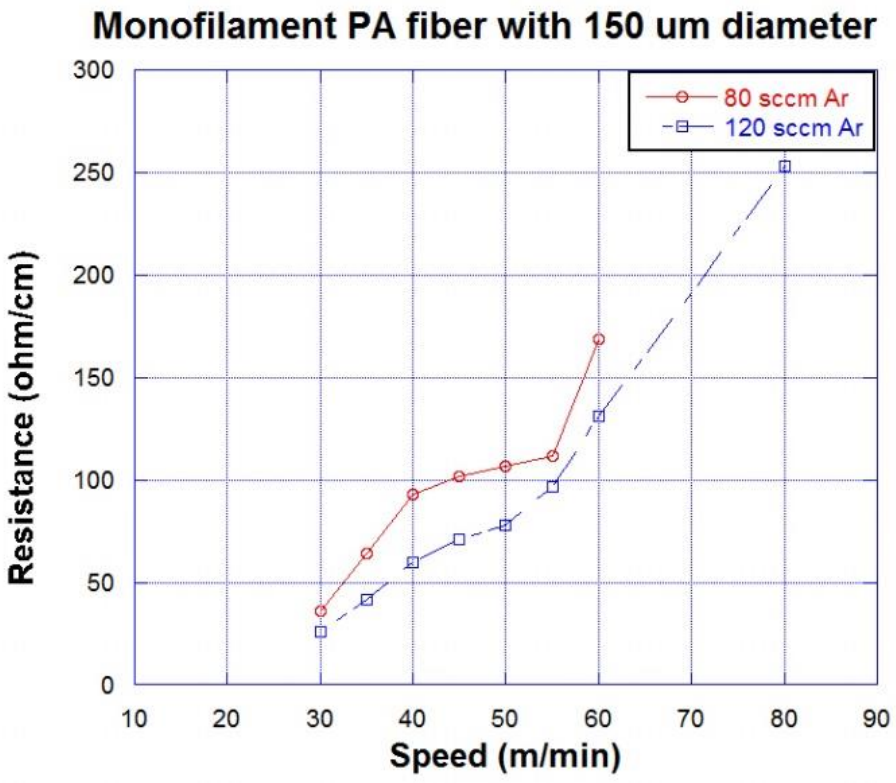

Figure 5.8. Electrical characterization plot of silver coated fiber with 150 um diameter

These two tables and graphs illustrate the resistance of fibers versus deposition speed of the thin film growth on them. It is clearly seen that resistance of metalized fibers increases with increase in deposition speed as expected. Because there is less deposition on fibers if deposition speed increases. On the other hand, the differences was observed between the results between 80 sccm and 120 sccm values. Higher gas flow increases the number of collisions and ionization which is resulted in increase in deposition rate. This occurrence increase the growth on fibers, that's why the results belong to 120 sccm have less resistance than the results belong to 80 sccm. It is also seen that there occur more growth of thin film on higher diameter when compared the graphs.

Table 5.10. Electrical characterization data of silver coated fiber with 85 um

d=85 um	**120 sccm**	**80 sccm**
m/min	**R(Ω/cm)**	**R(Ω/cm)**
20	NA	67
30	56	91
35	70	118
40	89	142
45	114	172
50	139	191
55	202	216
60	263	319

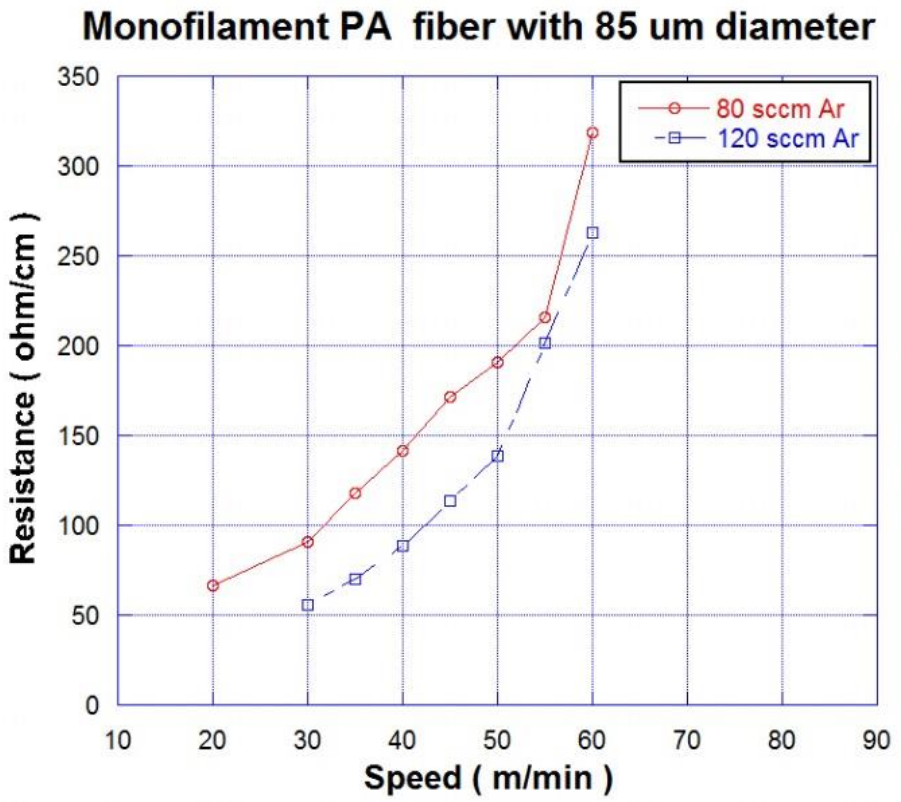

Figure 5.9. Electrical characterization graph of silver coated 150 um diametric fiber

5.7. Thin Film Thickness Measurements

5.7.1. Calculating from Measured Resistance

To procede these analysis, bulk resistivity formula was driven by using unknown parameter which was coated silver's cross section. Thickness was tried to obtain by coated silver's cross section. When all parameters were put into equation 4.3, it yielded thickness value by exact volume of thin, cylindrical, assuming hollow deposited structure on the fiber surface. As seen from the SEM images, there is no perfect hallow thin film deposition on PA fiber so there occur fallibility for the calculated result mathematically. Besides all, thin film on the PA fiber has cracks and roughness which cause wrong calculation from the real value. These factors were taken into consideration in order to reach optimized thickness.

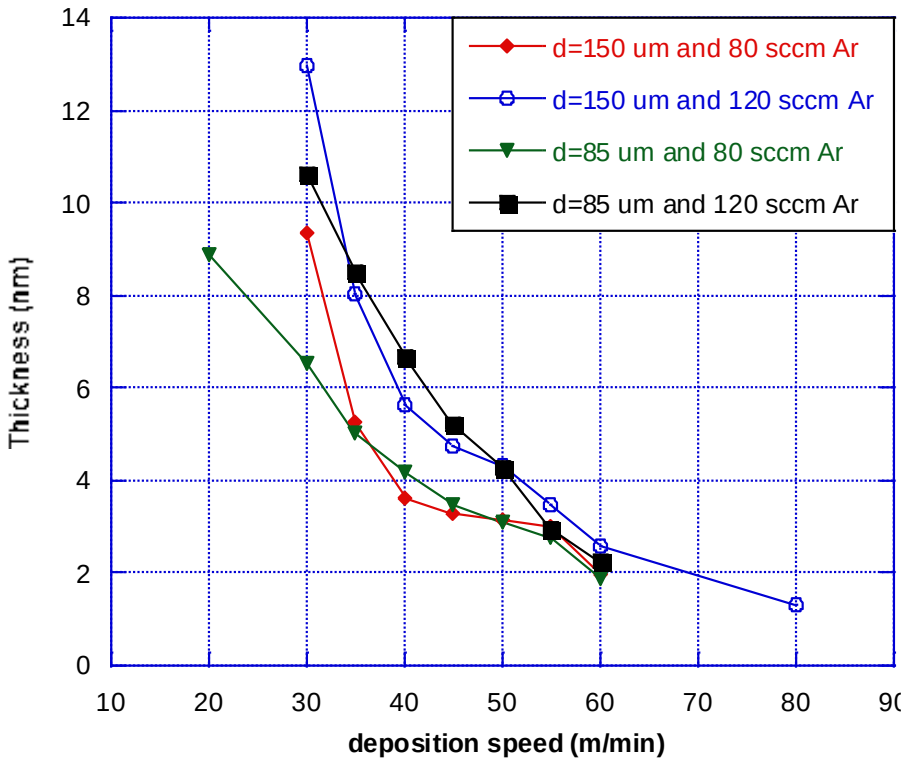

Figure 5.10. Deposition speed and thickness

Table 5.11. Numerical data of Figure 5.10

Deposition speed (m/min)	Thickness (nm) d=150 um and 80 sccm Ar	Thickness (nm) d=150 um and 120 sccm Ar	Thickness (nm) d=85 um and 80 sccm Ar	Thickness (nm) d=85 um and 120 sccm Ar
20	NA	NA	8.887	NA
30	9.372	12.977	6.5432	10.633
35	5.272	8.0335	5.046	8.5061
40	3.628	5.6235	4.1931	6.6902
45	3.308	4.7522	3.4618	5.223
50	3.153	4.3257	3.1174	4.2836
55	3.013	3.4784	2.7566	2.9477
60	1.996	2.5756	1.8665	2.264
80	NA	1.3336	NA	NA

Figure 5.10 present the relation between deposition speed and thickness of silver thin film on PA fibers. Graph obviously shows that thickness decreases with increase in deposition speed. By changing the deposition speed, desired thickness can be obtained. It is clearly seen that the change of resistance depends on the fiber speed that effects deposited film thickness.

5.7.2. Calculating from Deposited Silver Mass

Density formula was driven because pure silver density is known. We also get the volume of coated silver. The volume of the thin film is calculated by surface area of the 10 meter of fiber multiplied with thickness of thin film. The film thickness is so small, so that volume actually gives coating area. PA fiber with 150 um diameter at 30 m/min deposition speed was calculated to be deposited 320 nm thickness. PA fiber with 85 um diameter at same deposition speed has 101 nm thickness value. These calculations were done for hollow deposition on PA fibers but there were no perfect and homogenous

5.7.3. Calculating from Calibration Sample

In this part, glass lamella was deposited silver thin film and the thickness was measured with a surface profilometer. The rest of the data were evaluated according to this value. It can be seen from the graph that there is same decrease line when compared to the graph in calculating from measured resistance part which represents the relation between thickness and deposition speed. Glass lamella was used because thickness of deposited thin film can be measured by a surface profilometer which is convenient only for flat surface. The fact that glass lamella and PA fiber have different bonding structure and surface property that theirs surface allow different amount of deposition in other speech different thickness of grown thin film by same sputtering parameters. These differences were taken into consideration for thickness optimization part. Table 5.12 shows data of thickness measurement by calibration sample and Figure 5.11 shows resulted graph of this analysis.

Table 5.12. Thickness measurement data by calibration sample

Deposition Speed (m/min)	Thickness (nm)
20	96.6
30	64.4
35	55.2
40	48.3
45	42.9
50	38.6
55	35.1
60	32.2
80	24.1

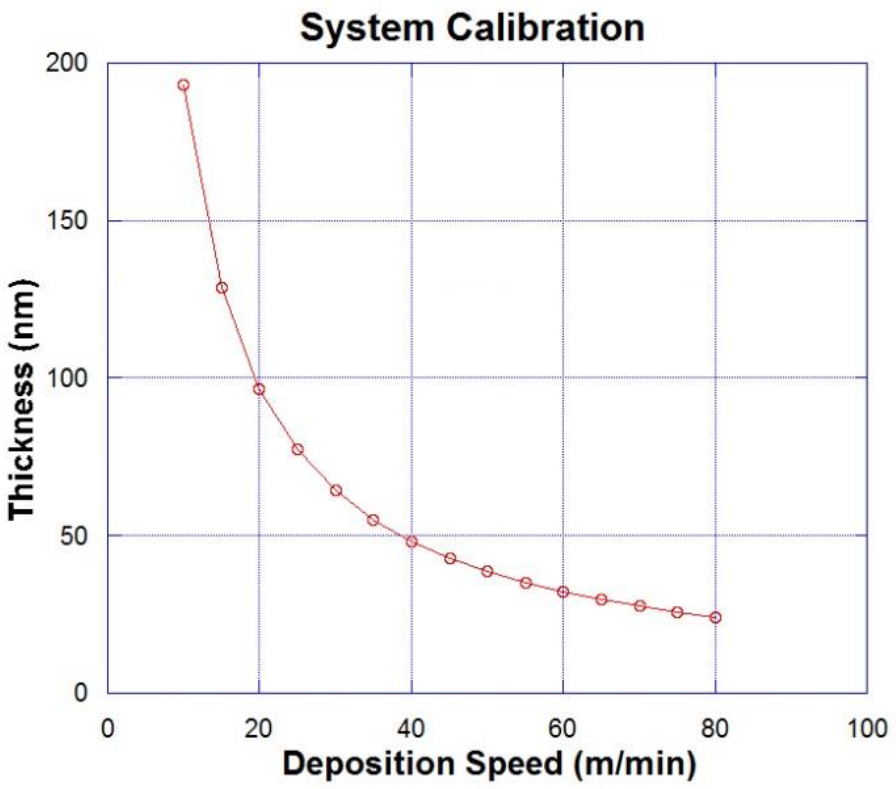

Figure 5.11. System calibration by coated glass lamella sample

5.7.4. Optimization of the Film Thickness

Three different method were driven to find optimum thickness of silver thin film but all values are different from each other. Firstly, calculating thickness from measured resistance do not represent the actual values because thickness values were not compatible with measurement in deposited silver mass.The result can be attributed to that the thickness is less than the mean free path of silver and the external surfaces scattering is the main factor! As explained at Section 3.10, resistance would be measured higher due to electrons scattering resulted surface or grain boundary scattering due to mechanical deformation. The following methods are also not reliable because there observed surface cracks on thin film on fiber by SEM analysis. The optimum value of the thickness can be found by making assumption between values found in calculating thickness from deposited silver mass section and thickness from calibration sample section. The mean free path of bulk silver which is 52 nm can lead to reasonable the optimum value. Let's call a K to be optimum value which is the order of thickness and mean free path. According to this assumption optimum coating thickness should be 100 nm in average.

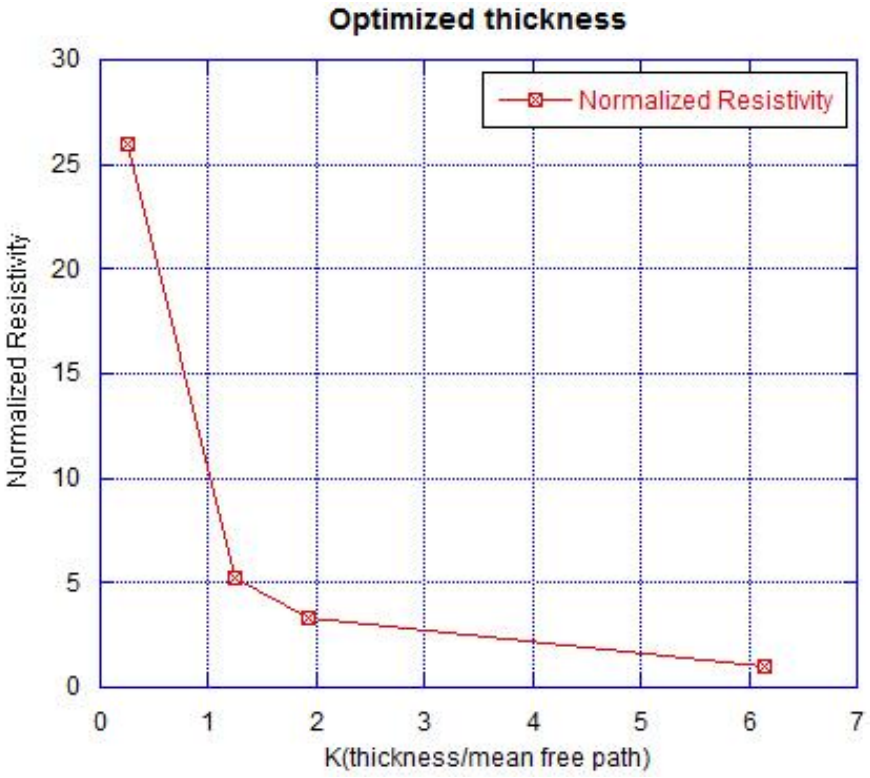

Figure 5.12. Optimized thickness

5.8. Antistatic

Antistatic property of woven fabrics regarding to surface resistance was investigated according to TS EN 1149-3 test standard. 12 fibers with different values of resistance were chosen and woven by sewing machine into fabrics. Sewing machine might have deformed thin film on the fiber and produced cracks on the surface so fiber resistance and surface resistance of fabrics proportionality may not continue. However, fabric surface resistance and fiber resistance are proportional when fabrics are separated according to employed gas flow during sputtering on fiber which were woven into them. In that way, surface resistance of fabrics increases with increase in fiber resistance implying to increase in deposition speed.

Table 5.13. Antistatic property of metalized fibers woven into fabrics

Fiber diameter (um)	Gas flow (sccm)	Deposition speed (m/min)	Fiber resistance (ohm/cm)	Surface resistance of fabric (k.ohm/sq)
150	80	30	36	13.6
150	80	45	102	45.6
150	80	60	169	158
150	120	35	42	30.6
150	120	45	71	40.2
150	120	60	137	44.2
85	80	30	91	52.2
85	80	45	172	136
85	80	60	319	378
85	120	30	56	25.2
85	120	40	88	51.7
85	120	60	263	244.2

Surface resistance of fabrics are in conducting and shielding range which is around kohm. To obtain antistatic value, surface resistance should be at least around 1 Gohm values. The data were received from unwashed fabrics but washing increases surface resistance of fabrics. Furthermore, antistatic value were reached by washing process operated with washing machine. Further details like standard deviation or antistatic values can be observed at adhesion tests part.

5.9. Shielding

Fabrics which were used in antistatic test were also employed for TS EN 1149-1 shielding test standard. It says that obtained shielding factors should approach to 1 for fabrics to be claimed to possess shielding property. Unwashed fabrics were observed to have shielding property because shielding factors are very close to 1. Shielding factor and surface resistance proportionality were not observed. It can be resulted due to the cracks on the thin film or damage due to sewing machine. Another reason can be misorientation of conductive fibers lines obtained by sewing machine.

Table 5.14. Shielding property of metalized fibers woven into fabrics

Fiber diameter (um)	Deposition speed (m/min)	Fiber resistance (ohm/cm)	Surface resistance of fabric (kohm/sq)	Shielding factor
150	30	36	13.6	0.975
150	45	102	45.6	0.94
150	60	169	158	0.96
150	35	42	30.6	0.98
150	45	71	40.2	0.97
150	60	137	44.2	0.83
85	30	91	52.2	0.94
85	45	172	136	0.86
85	60	319	378	0.85
85	30	56	25.2	0.935
85	40	88	51.7	0.95
85	60	263	244.2	0.974
	at 80 sccm gas flow			
	at 120 sccm gas flow			

5.10. Adhesion Tests

Table 5.15. Surface resistance and washing durability relation data of the fabrics

Fiber Resistance (ohm/cm)	**For 5 samples each fabrics**	**Surface Resistance**			
		Unwashed	**After 10 wash**	**After 20 wash**	**After 30 wash**
		kohm/sq	**Gohm/sq**	**Gohm/sq**	**Gohm/sq**
36	**Avg:**	13.6	12.81	22.12	90.04
	Std_dev:	0.92	2.77	0.96	3.19
102	**Avg:**	45.6	12.04	25.56	84.78
	Std_dev:	0.58	0.70	0.78	7.59
169	**Avg:**	158	8.872	23.86	99.36
	Std_dev:	13.57	0.22	0.95	15.71
42	**Avg:**	30.6	9.604	29.94	91.58
	Std_dev:	06.34	0.74	4.30	5.37
71	**Avg:**	40.2	28.1	30.42	96.36
	Std_dev:	07.53	5.01	1.80	0.65
137	**Avg:**	44.2	8.136	23.94	127.8
	Std_dev:	08.53	0.69	1.21	13.21
91	**Avg:**	52.2	11.16	23.68	165
	Std_dev:	06.23	0.82	1.23	6.04
172	**Avg:**	136	7.698	26.06	95.56
	Std_dev:	10.30	0.27	2.01	1.55
319	**Avg:**	378	9.94	32.24	119.8
	Std_dev:	32.66	0.72	1.44	10.98
56	**Avg:**	25.2	8.466	31.08	124.2
	Std_dev:	0.78	0.33	4.78	8.31
88	**Avg:**	51.7	24.5	26.86	78.2
	Std_dev:	2.74	3.18	1.71	1.46
263	**Avg:**	244.2	11.72	23.46	173.2
	Std_dev:	10.18	0.65	1.33	28.77

	at 80 sccm gas flow
	at 120 sccm gas flow

The italic and bold character of fiber resistance represent fiber with 150 um in diameter and other values of the fiber resistance represent 85 um diametric fibers.

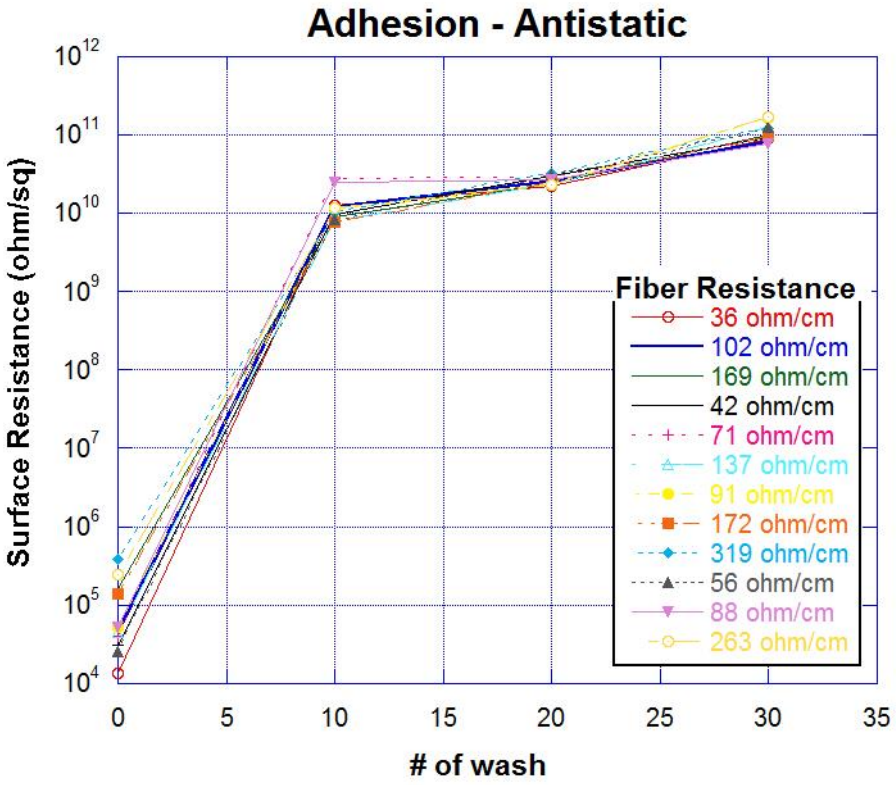

Figure 5.13. Surface resistance and washing durability relation of fabrics

Initially the surface rsistivity of unwashed and unwoven of the fabric was measured 147 Gohm/sq. The facrics used in antistatic and shielding property investigation were washed by a classic washing machine. Surface resistance were measured in 10 wash interval and re-measured. It was observed that number of wash increases the surface resistance. A great increase was observed from kohm to Gohm in surface resistance after first 10 wash and then values raised slowly. Although fibers have different resistance, their surface resistance values aproach each other after washing. The graphs show that, mechanical durability of thin film to classical washing proocess is very weak for first 10 wash but it remains durable after other 10 washs. The measurement periodicity was taken 10 wash so that it is not clear weather the change was occurred at first wash or near to 10 wash. It is believed that fabric surface resistance would be sharply increased by fiirst wash and the change rate would remain same with 10 wash and others. I seems that these fabrics can be remain antistatic up to 30 wash. After 30 wash, fabrics were turned to unwashed and unwoven surface resistance value. Relative humudity(RH) is an important

factor to pay attention during these measurements . In this research, RH was considered to be constatnt for evry measurement.

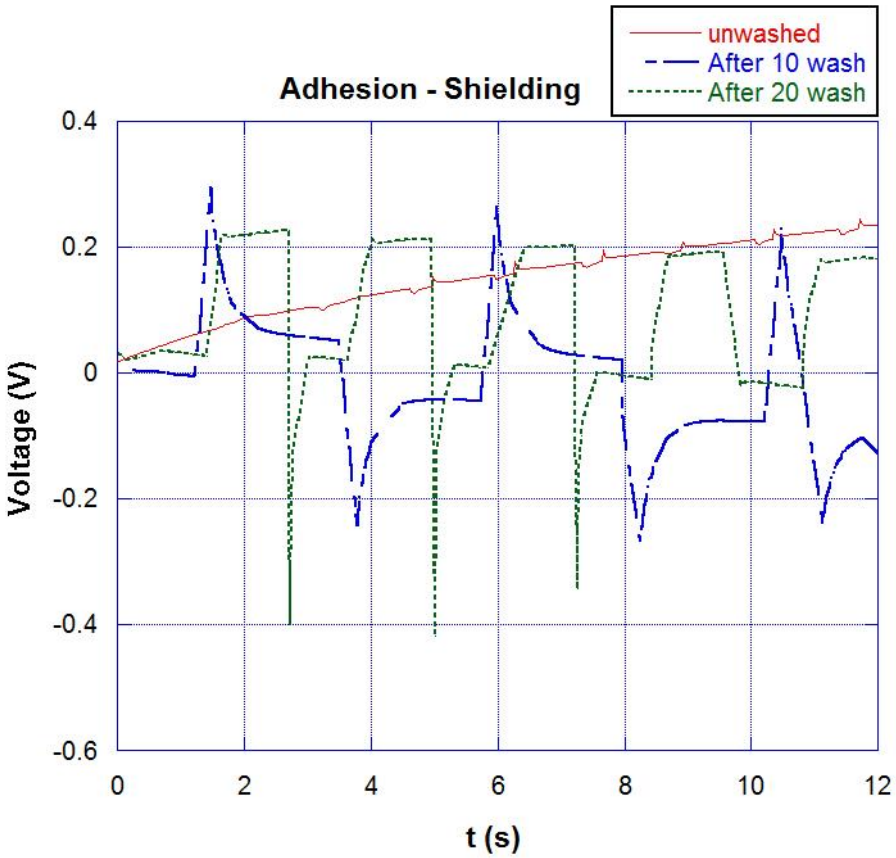

Figure 5.14. Shielding property and washing durability relation of fabrics

One of the fabric was chosen to analyze the washing durability of silver thin film by shielding property measurement. The fabrics having woven by 36 ohm/cm resistance fiber and initially with 13.6 kohm/sq surface resistance was employed. Unwashed fabric was observed to have good shielding value and fast charge decay capability in 0.1 second. Charge decay time were slowed down in 2 or 3 seconds after 10 wash of fabrics. Fabric were washed 20 times and then, shielding factor of fabric was remeasured. Fabric was showed nearly no shielding property and charge decay. As a matter fact that fabrics was behaved as insulator with respect to shielding property.

CHAPTER 6

CONCLUSIONS

Developments in nanotechnology enable textile industry to produce smart, healthy, safe, sensitive and functional textile materials. Fibers processed with nanoparticles, thin films technology and nanocomposites offers various applications in functional textile products. Thin film technology is widely used to functionalize the textile materials by surface finishing or thin film growth on polymer fibers. In this research, fabrics were aimed to promote antistatic property which capable to control electrostatic charge shearing safely and to prevent static charge accumulation on surface.

A new inverted cylindrical magnetron sputtering system were designed to growth silver thin film on all sides of polyamide fibers to serve the aim of this research. This design enabled to growth silver in high deposition speed and fiber to make more cycles through plasma comparing to our previous system. A roll to roll mechanism mounted to the system and provided to deposit silver thin film on PA fibers continuously at high deposition speed. Two 99.999 % pure and ring shaped silver targets were employed at the same time. System were optimized for several sputtering parameters such as; diameters of fibers, their number of cycles through the plasma, gas flow, deposition speed and applied power for coated fiber production in industrial scale range. Obtained fibers were characterized by electrical, optical, morphological and microstructural analysis.

The most efficient deposition distance for substrates was found 3.3 cm target to substrate distance for ring shaped target possessed 5.3 cm radius. 150 and 85 um diametric PA fibers were chosen as substrates and they were placed in the system so that they do 35 cycles through system. 80 sccm gas flow was discovered to be lower limit to sustain plasma in our ICM system and 120 sccm gas flow was also studied as sputtering parameters. The lowest limit of deposition speed was discovered as 20 m/min and the highest deposition speed was discovered to be 80 m/min. Optimum applied power was discovered as 140 watt for each target and power remained same for all deposition.

Optical microscopy analysis show that good homogeneity and no roughness on silver thin film for both 85 and 150 um diametric PA fibers. SEM characterizations gave

good results for silver composition and homogeneity however, some cracks and little roughness were encountered on thin film especially on 85 um diametric fiber. XRD characterization was investigated, and (111) and (200) peaks were obtained clearly same from the literature as explained.

In order to obtain thickness of fibers, they are employed three different methods, all results were compared to find optimum thickness. Optimum thickness were assumed as 100 nm (see Section 5.7). It is clearly understood from the electrical study that resistance of metalized fibers increases with increase in deposition speed as expected. Because there is less deposition on fibers if deposition speed increases which means that grown thin film has less thickness. Higher gas flow increases the number of collisions and ionization which is resulted in increase in deposition rate. It is also seen that there occur more growth of thin film on higher diametered fiber when compared the graphs.

Metalized fibers were woven into a synthetic fabrics to promote them antistatic property. Fibers were woven in 10 mm interval lines apart from each other horizontal and vertical in a 35 cm X 35 cm synthetic fabrics which originally have 147 Gohm/sq surface resistance. Twelve fabrics were woven by fibers whose resistance varied from 36 ohm/cm to 319 ohm/cm. Surface resistance of these 12 fabrics varied from 13.6 kohm/sq to 378 kohm/sq. These results were in the range of shielding materials. Fabrics can be interpreted to be good shielding property.

The adhesion analysis of these fabrics were carried out by conventional washing process. Shielding and surface resistance of the fabrics were re-measured after each 10 wash and compared to each other. Surface resistance raised to Gohm which satisfy antistatic property and it is observed that these fabrics were durable more than 30 wash to maintain antistatic property. Fabrics originally having surface resistance 13.6 kohm/sq and resulted charge decay in 0.1 second which can be claimed to have good shielding property. Washing 10 times affected this fabric charge decay time to be more than 2 second and after 20 wash shielding property was disappeared.

Finally, silver thin film was successfully and homogeneously coated on polyamide fibers at high deposition speed by roll to roll ICM system. Antistatic fabrics were obtained by these fibers and results show that silver thin film is durable for 30 wash to satisfy antistatics propery. These research satisfied the expectations from functional and technique textile products in terms of shielding and antistatic properties.

REFERENCES

Adanur, S., Y. Mogahzy, and F. Abdel-Hady. 2001. Yarn and Fabric Design and Analysis in 3D Virtual Reality. *National Textile Center Research Briefs–Integrated Enterprise Systems Competency*:95-96.

Amberg, M., J. Geerk, M. Keller, and A. Fischer. 2004. Design, characterisation and operation of an inverted cylindrical magnetron for metal deposition. *Plasma Devices and Operations*. 12:175-186.

Andersson, J., P. Ni, and A. Anders. 2013. Spectroscopic imaging of self-organization in high power impulse magnetron sputtering plasmas. *Applied Physics Letters*. 103:054104.

Baghriche, O., C. Ruales, R. Sanjines, C. Pulgarin, A. Zertal, I. Stolitchnov, and J. Kiwi. 2012. Ag-surfaces sputtered by DC and pulsed DC-magnetron sputtering effective in bacterial inactivation: testing and characterization. *Surface and Coatings Technology*. 206:2410-2416.

Bajaj, P., A. Gupta, and N. Ojha. 2000. Antistatic and hydrophilic synthetic fibers: A critique. *Journal of Macromolecular Science, Part C: Polymer Reviews*. 40:105-138.

Benn, T.M., and P. Westerhoff. 2008. Nanoparticle silver released into water from commercially available sock fabrics. *Environmental science & technology*. 42:4133-4139.

Bhat, M.A., and V. Kumar. 2013. Calculation of SAR and Measurement of Temperature Change of Human Head Due To The Mobile Phone Waves At Frequencies 900 MHz and 1800 MHz. *Advances in Physics Theories and Applications*. 16:54-63.

Bhushan, N.L. 2011. Injuries, Illnesses, and Fatalities in Food Manufacturing, 2008. *Available on line at: http://www. bls. gov/opub/cwc/sh20110118ar01p1. htm. Accessed May*. 6:2011.

Black, S., Kapsali, V., Bougourd, J., & Geesin, F. (2005). Fashion and function: factors affecting the design and use of protective clothing. *Textiles for protection.*

Bosetti, M., A. Masse, E. Tobin, and M. Cannas. 2002. Silver coated materials for external fixation devices: in vitro biocompatibility and genotoxicity. *Biomaterials*. 23:887-892.

Böhlmark, Johan. "Fundamentals of high power impulse magnetron sputtering." (2006), *(Linköping Studies in Science and Technology, Dissertation No. 1014)*

Brydson, J.A. 1999. Plastics materials (7th Ed.). Butterworth-Heinemann, *ISBN: 978-0-7506-4132-6*

Callister, W.D., and D.G. Rethwisch. 2007. Materials science and engineering: an introduction (7th Ed.). *Wiley New York, ISBN-13: 978-0-471-73696-7*

"Carbon atom", last modified Sebtember, 13, 2013, *http://bc.outcrop.org/GEOL_B10/lecture5.htm*l

Chaloupka, K., Y. Malam, and A.M. Seifalian. 2010. Nanosilver as a new generation of nanoproduct in biomedical applications. *Trends in biotechnology*. 28:580-588.

Chandra, A., L.-S. Turng, K. Li, and H.-X. Huang. 2011. Fracture behavior and optical properties of melt compounded semi-transparent polycarbonate (PC)/alumina nanocomposites. *Composites Part A: Applied Science and Manufacturing*. 42:1903-1909.

Chapman, B.N. 1980. Glow discharge processes. *Wiley, New York*.

Chen, F.F., and M.D. Smith. 1984. Plasma. *Wiley Online Library*.

Chen, M., X. Bai, J. Gong, C. Sun, R. Huang, and L. Wen. 2000. Properties of reactive magnetron sputtered ITO films without in-situ substrate heating and post-deposition annealing. *J. Mater. Sci. Technol., Vol.16 No.3*.

Chen, Y.-H., C.-C. Hsu, and J.-L. He. 2013. Antibacterial silver coating on poly (ethylene terephthalate) fabric by using high power impulse magnetron sputtering. *Surface and Coatings Technology*. 232:868-875.

"CVD method" last modified January 2, 2014, *http://www.azonano.com/article.aspx?ArticleID=3423*

Dowling, D., K. Donnelly, M. McConnell, R. Eloy, and M. Arnaud. 2001. Deposition of anti-bacterial silver coatings on polymeric substrates. *Thin Solid Films*. 398:602-606.

Drake, P.L., and K.J. Hazelwood. 2005. Exposure-related health effects of silver and silver compounds: a review. *Annals of Occupational Hygiene*. 49:575-585.

"Dual HIPIMS" last modified 2014, *http://pag.lbl.gov/Research-Topics/srf-cavities*

Dubas, S.T., P. Kumlangdudsana, and P. Potiyaraj. 2006. Layer-by-layer deposition of antimicrobial silver nanoparticles on textile fibers. *Colloids and Surfaces A: Physicochemical and Engineering Aspects*. 289:105-109.

"Explosion due to ESD" last modified 2011, *http://www.esdjournal.com/static/Georgia/georgia%20sugar%20explosion.htm*

"Evaporation" last modified 2011, *http://uwcourseplanner.com/calendar/NE/343/*

"e-beam evaporation " last modified October, 2014, *http://thermalcoatng.com/vacuum-coating-thermal-evaporation/"*

"E-Field lines" last modified 2013, *http://www.wwk.in/physics/electricity-and-magnetism/electric-field*

Farrell, W., P. Smith, G. Delory, G. Hillard, J. Marshall, D. Catling, M. Hecht, D. Tratt, N. Renno, and M. Desch. 2004. Electric and magnetic signatures of dust devils from the 2000–2001 Matador desert tests. *Journal of Geophysical Research: Planets (1991–2012)*. 109.

Francombe, M.H., and J.L. Vossen. 1992. Physics of thin films, *Akademic Press.*

Fruton, J.S. 2002. A history of pepsin and related enzymes. *The Quarterly review of biology*. 77:127-147.

Groop, E., A. Nowicki, C. Calle, C. Buhler, and J. Mantovani. 2003. Comparison of surface resistivity and triboelectric charge generation characteristics of materials. *In Proceedings of the 40th Space Congress. 6.*

Guimond, S., B. Hanselmann, M. Amberg, and D. Hegemann. 2010. Plasma functionalization of textiles: specifics and possibilities. *Pure and Applied Chemistry*. 82:1239-1245.

Hasegawa, Y., M. Shikida, D. Ogura, Y. Suzuki, and K. Sato. 2008. Fabrication of a wearable fabric tactile sensor produced by artificial hollow fiber. *Journal of micromechanics and microengineering*. 18:085014.

Hausmann, K. 2007. Permanent antistatic agent offers long term performance for films and containers. *Plastics, Additives and Compounding*. 9:40-42.

Hegemann, D., M.M. Hossain, and D.J. Balazs. 2007. Nanostructured plasma coatings to obtain multifunctional textile surfaces. *Progress in organic coatings*. 58:237-240.

Heine, E., H. Knops, K. Schaefer, P. Vangeyte, and M. Moeller. 2007. Antimicrobial Functionalisation of Textile Materials. *Multifunctional barriers for flexible structures: textile, leather and paper. Springer Series in Materials Science*:23-37.

"IC threshold values", last modified September 14, 2014, *http://4g.net.tr/v1/?p=166*

Jahn, R.G. 2012. Physics of electric propulsion. *Courier Dover Publications.*

James, M., L. Wilson, S. Lane, J. Gilbert, T. Mather, R. Harrison, and R. Martin. 2008. Electrical charging of volcanic plumes. *In* Planetary Atmospheric Electricity. *Springer. 399-418.*

Jiang, S., W. Qin, R. Guo, and L. Zhang. 2010. Surface functionalization of nanostructured silver-coated polyester fabric by magnetron sputtering. *Surface and Coatings Technology*. 204:3662-3667.

Kaynak, H.K., and O. Babaarslan. 2011. Mikrofilament İnceliğinin Dokuma Kumaş Özelliklerine Etkisi. *Tekstil Teknolojileri Elektronik Dergisi*. 5:30-39.

Kern, W. 1991. Thin film processes II. *Academic press*.

Körner, E., P. Rupper, J.F. Lübben, A. Ritter, J. Rühe, and D. Hegemann. 2011. Surface topography, morphology and functionality of silver containing plasma polymer nanocomposites. *Surface and Coatings Technology*. 205:2978-2984.

Lacasse, K., and W. Baumann. 2004. Textile Chemicals: Environmental data and facts. *Springer*.

Latham, J., and C. Stow. 1969. Airborne studies of the electrical properties of large convective clouds. *Quarterly Journal of the Royal Meteorological Society*. 95:486-500.

Lieberman, M.A., and A.J. Lichtenberg. 1994. Principles of plasma discharges and materials processing. *MRS Bulletin*. 30:899-901.

Lorenz, C., L. Windler, N. Von Goetz, R. Lehmann, M. Schuppler, K. Hungerbühler, M. Heuberger, and B. Nowack. 2012. Characterization of silver release from commercially available functional (nano) textiles. *Chemosphere*. 89:817-824.

Luo, W., and X. Zheng. A Model of Size Effect on Thermal Conductivity for Thin Metallic Films, *PIERS Proceedings, Xi'an, China, March 22–26, 2010*.

Martinez, F. 2014. Explosive Safety with Regards to Electrostatic Discharge, *Doctoral dissertation.*

McGuire, G., D. Temple, M. Ray, D. Dausch, and M. Lamvik. 1999. Ion beam sputter deposition of low work function and GMR materials. *Superficies y vacío*. 8:1-3.

Meriç, Z. 2011. Antistatic applications: Metal coated fibers by magnetron sputtering, *M.Sc. Thesis, İzmir Institute of Technology*

Ohring, M. 2001. Materials science of thin films. *Academic press.*

Onar, N., M.F. Ebeoglugil, I. Kayatekin, and E. Celik. 2007. Low-temperature, sol–gel-synthesized, silver-doped titanium oxide coatings to improve ultraviolet-blocking properties for cotton fabrics. *Journal of applied polymer science*. 106:514-525.

Özyüzer, L., Z. Meriç, Y. Selamet, B. Kutlu, and A. Cireli. 2010. Antistatic and Antibacterial Properties of Metal Coated Polypropylene Fibers by Magnetron Sputtering. *The Journal of Textiles and Engineers, 2010 (Volume: 17)*. 78.

Pang, E.C., and W. Chow. 2012. Fire Safety Concerns on Residential Areas Located Adjacent to Oil Tanks. *Journal of Applied Fire Science*. 22:223-238.

Powell, R., and A. Ulman. 1999. Ionized physical vapor deposition. *Academic Press.*

"Resistivity in materials " January 15, 2015, *http://en.wikipedia.org/wiki/Electrical_resistivity_and_conductivity*

"Rf sputtering" last modified 2011, *http://uwcourseplanner.com/calendar/NE/343/*

Scholz, F., and U. Hasse. 2005. Controlling the morphology of silver deposition at liquid| liquid interfaces: From nano-wires to super smooth films. *Electrochemistry communications*. 7:541-546.

Sekhon, B.S. 2010. Food nanotechnology–an overview. *Nanotechnology, science and applications*. 3:1.

Sizing, T., and M. Dekker. 2013. Institute of Biopolymers and Chemical Fibres. *Fibres & Textiles in Eastern Europe*. 21:101.

Süpüren, G., N. Oglakcioglu, N. Ozdil, and A. Marmarali. 2011. Moisture management and thermal absorptivity properties of double-face knitted fabrics. *Textile Research Journal*:0040517511402122.

"Thermal evaporation" last modified October 16, 2014, *http://nptel.ac.in/courses/115103039/module16/lec38/3.html*

Tuna, O., Y. Selamet, G. Aygun, and L. Ozyuzer. 2010. High quality ITO thin films grown by dc and RF sputtering without oxygen. *Journal of Physics D: Applied Physics*. 43:055402.

Venables, J. 2000. Introduction to surface and thin film processes. *Cambridge University Press.*

Vigneshwaran, N., A. Kathe, P. Varadarajan, R. Nachane, and R. Balasubramanya. 2007. Functional finishing of cotton fabrics using silver nanoparticles. *Journal of nanoscience and nanotechnology*. 7:1893-1897.

Wang, A.Z. 2002. On-chip ESD protection for integrated circuits: an IC design perspective. *Springer.*

Wang, S., L. Lin, and Z.L. Wang. 2012. Nanoscale triboelectric-effect-enabled energy conversion for sustainably powering portable electronics. *Nano letters*. 12:6339-6346.

Wessapan, T., S. Srisawatdhisukul, and P. Rattanadecho. 2011. Numerical analysis of specific absorption rate and heat transfer in the human body exposed to leakage electromagnetic field at 915 MHz and 2450 MHz. *Journal of Heat Transfer*. 133:051101.

"ESD interaction while walking", last modified April 10, 2001, *http://esdsystems.descoindustries.com/Newsletters/images*

Wilson, I.S., and J.J. Varela. 2014. Everything Safety: Technical Terms to ESD Experiments. *Los Alamos National Laboratory (LANL).*

Windler, L., M. Height, and B. Nowack. 2013. Comparative evaluation of antimicrobials for textile applications. *Environment international*. 53:62-73.

Yoosefi Booshehri, A., R. Wang, and R. Xu. 2013. The effect of re-generable silver nanoparticles/multi-walled carbon nanotubes coating on the antibacterial performance of hollow fiber membrane. *Chemical Engineering Journal*. 230:251-259.

Zhang, W.D., L. Shen, I.Y. Phang, and T. Liu. 2004. Carbon nanotubes reinforced nylon-6 composite prepared by simple melt-compounding. *Macromolecules*. 37:256-259.

Ziaja, J., J. Koprowska, and J. Janukiewicz. 2008. Using plasma metallisation for manufacture of textile screens against electromagnetic fields. *Fibres & Textiles in Eastern Europe*. 16:64-66.